CHAPTER V

RESULTS AND DISCUSSION

In this study, stochastic simulation of ambient PM_{10} concentration using Monte-Carlo method was carried out using two types of inputs with uncertainty, meteorological input and emission rate input. First, the suitability of the ISCST3 model was evaluated by comparing the model prediction on ambient concentration of PM_{10} against the actual data. Next the results of 50 repeated Monte-Carlo simulation using fifty random sets of statistically generated values for each uncertain input were statistically collected and analyzed to obtain the range of variation in PM_{10} concentration and the probability of PM_{10} concentration exceedance estimated at five different receptors in the study area.

5.1 Evaluation of the ISCST3 Model

In order to evaluate the ISCST3 model performance, the year 1996 was selected as base year because of the most completeness of the required meteorological data in the study area. All optional model parameters and their values, such as dry deposition with plume depletion, equivalent elevated Cartesian sources and receptor network were the same as those to be used in subsequent Monte-Carlo simulations. As for the fugitive dust emission inventory, the same set of U.S. EPA's emission factors for crushed stone processing was used along with the assumption that there were ineffective or no dust suppression systems in use.

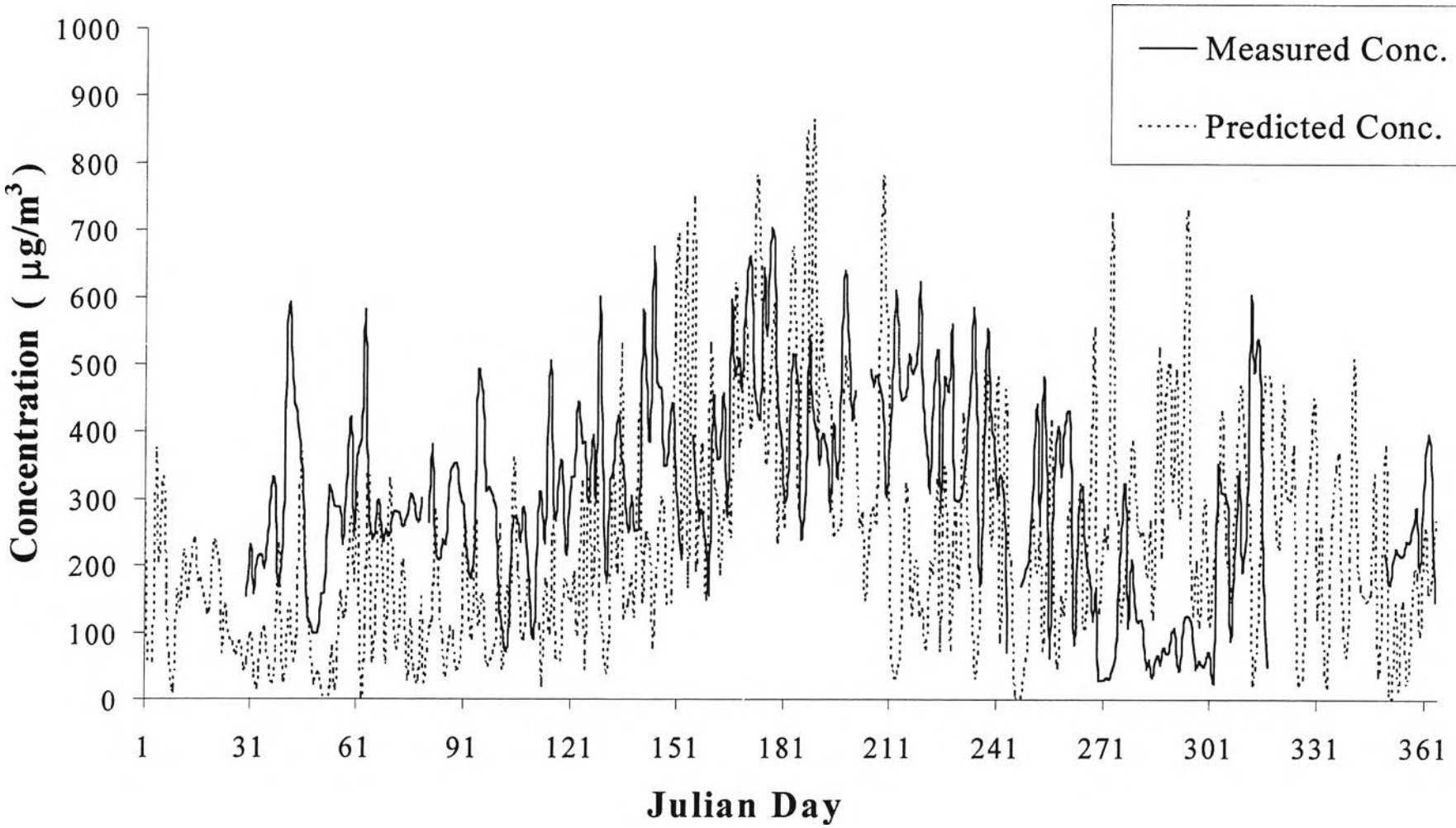

Figure 5.1 Comparison of 24-hr average concentrations of PM_{10} predicted by ISCST3 model *vs.* measurement at Na Pra Laan monitoring station of PCD in 1996.

Figure 5.1 compares the 24-hr average ambient concentration of PM_{10} predicted by the ISCST3 model at the ground level with the counterpart concentration measured at the monitoring station of PCD in Nah Pra Laan area. In Figure 5.1, the dashed line represents the 24-hr average concentration of PM_{10} predicted by the ISCST3 model, which was found most of the time to underestimate the measured data represented by the solid line. Nevertheless, the situation was found to reverse itself in some time episodes, particularly during the rainy season.

To focus on the above comparison in more details, two typical months, February and July, were selected to represent the dry and wet months, respectively. Figure 5.2 illustrates the 24-hr average PM_{10} concentrations recorded at the monitoring station and predicted by the ISCST3 model in February 1996. Obviously, the predicted values are lower than the observed most days of the month. Underestimation in the model results may be attributed to uncertainty in the emission data of multiple sources, in other words, actual stone-processing plant capacities. Because of lack of reliable data, the emission rates were calculated from the surveyed nominal plant capacity. In reality, the actual production capacity and the accompanying emission rates from each plant were not constant but varied upon the time of the day. The generation and dispersion of fugitive dust also depend on the local meteorological condition, such as wind direction, wind speed, ambient temperature, etc., as well as the moisture content of the feed materials. Because of lack of data, the present study assumed the emission rate of each plant remained constant throughout the 24 hours. In addition, a relatively high background value from other nearby sources, for instances, dust re-entrainment by road traffic, dust generated during transportation and construction activities not considered in the simulation can contribute to a significant difference between the predicted and measured concentration values.

Above all, the meteorological parameters, especially, the wind speed and direction, are known to play a great role in both the under- and over-estimation of fugitive dust concentration. Because of lack of wide-area wind speed and velocity data, there was no choice but to use the data recorded at the Nah Pra Laan station as the value for the whole study area.

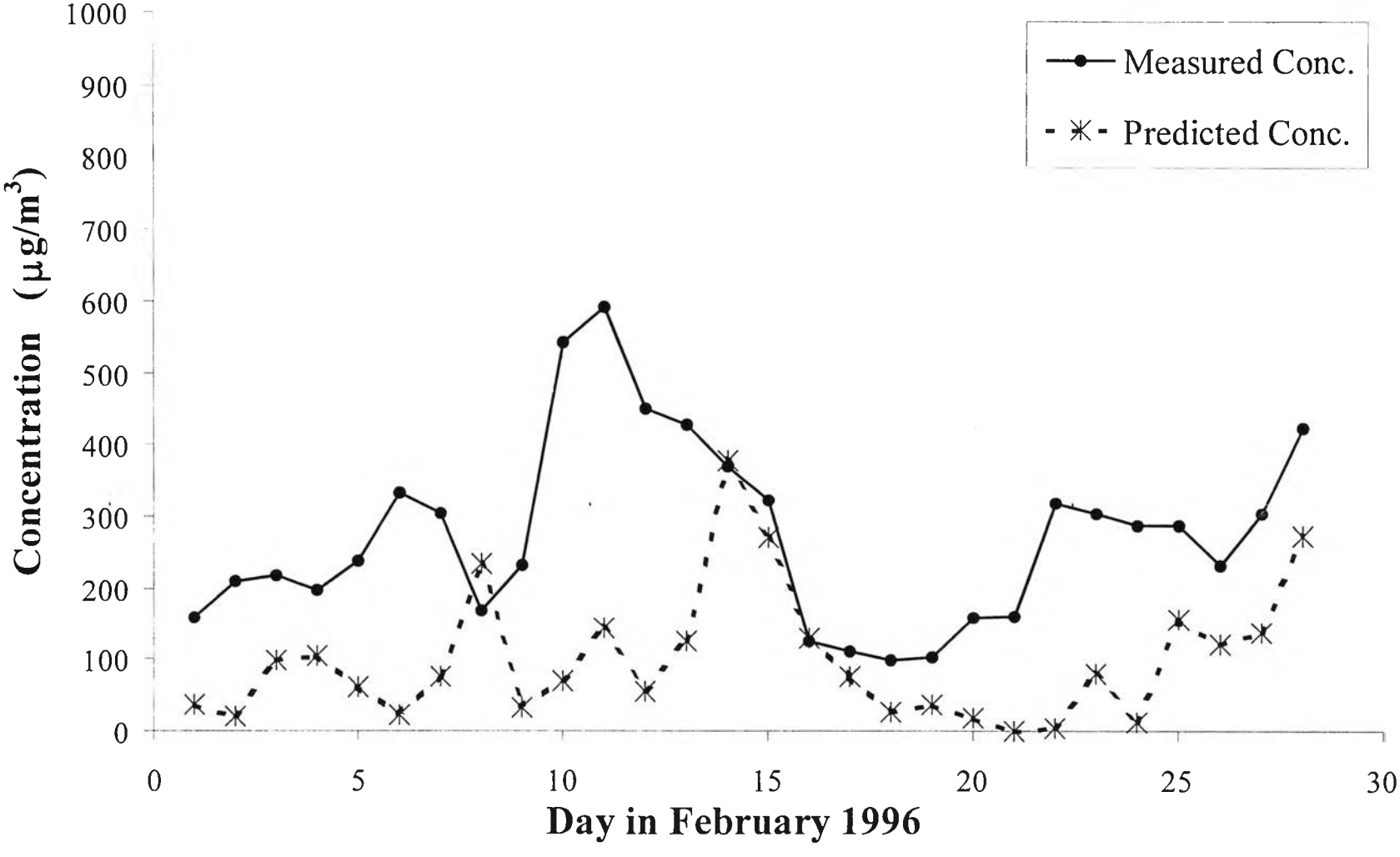

Figure 5.2 Comparison of 24-hr average concentrations of PM_{10} predicted by ISCST3 model *vs.* measurement at Na Pra Laan monitoring station of PCD in February 1996.

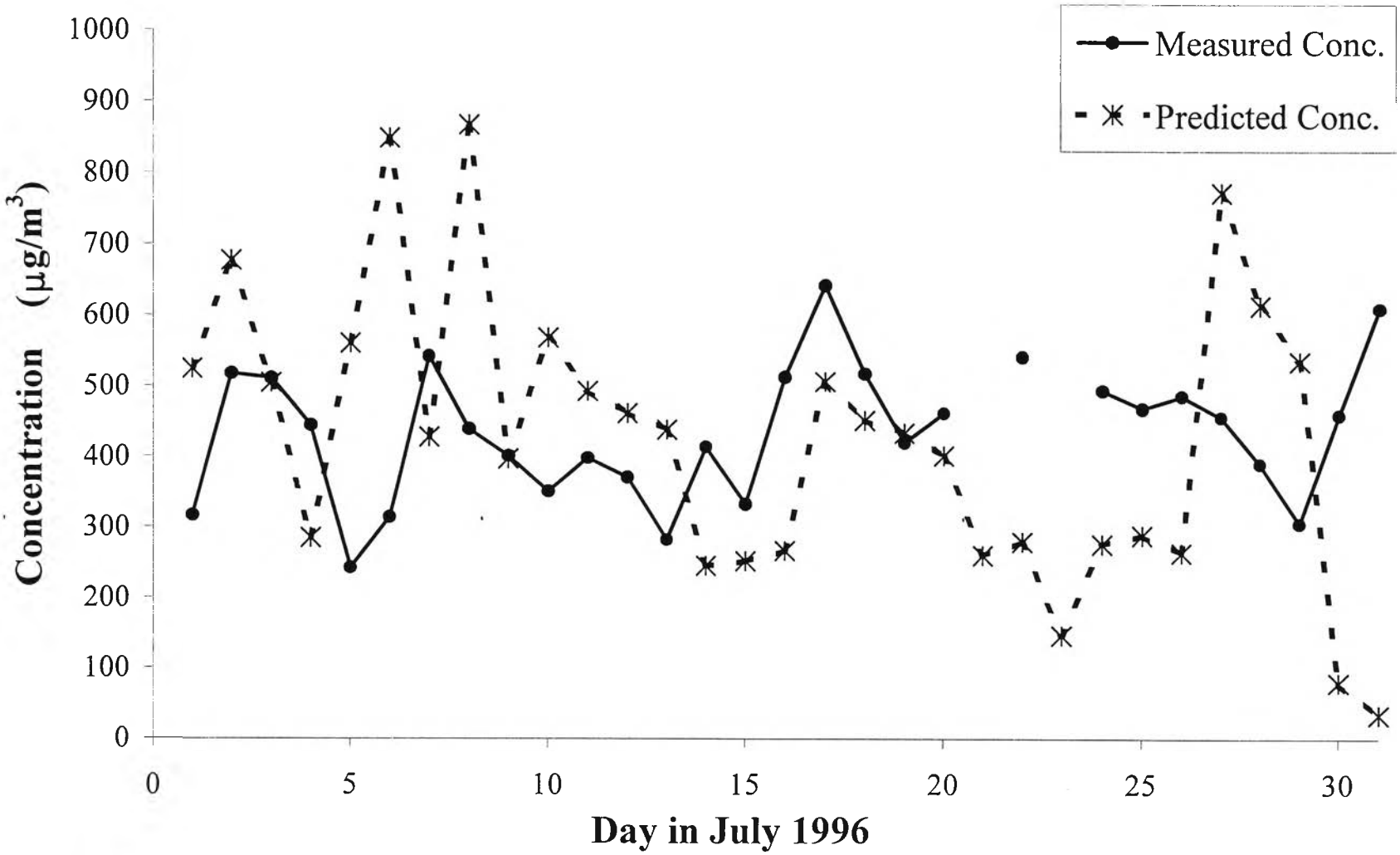

Figure 5.3 Comparison of 24-hr average concentrations of Pm_{10} predicted by ISCST3 model *vs*. measurement at Na Pra Laan monitoring station of PCD in July 1996.

On the other hand, Figure 5.3 shows that several overestimation of the daily average PM_{10} concentration occured in July 1996 that might be attributed to the scavenging effect caused by brief bursts of heavy rainfalls. As can be expected, the average PM_{10} concentrations in the rainy season tended to be lower than those in the dry season because of the additional effect of wet precipitation, which was not taken into account in the simulation. Moreover, it is known that the higher the moisture content of stone, the lower the dust generation rate becomes.

Nevertheless, the discrepancy between the predicted and observed daily average concentration and its cause may be summarized as follows:

1) As mentioned above, the background PM_{10} concentration values belonging to other nearby sources, for instance, transportation road dust re-entrainment, construction activities, etc., were not considered because surveyed data of source distributions were not available and difficult to collect. Therefore, the measured concentrations appeared to be higher than the predicted ones most of the time, particularly, in the summer months (March - May) and winter months (December – February) because of little rainfall.
2) Another major factor causing the discrepancy between the measured and predicted concentrations is the uncertainty in some meteorological data, which are strongly influenced by geographical location and local topography. In addition, this study assumed the meteorological data to be constant over every hour despite inevitable fluctuation against time. By the way, no local data on the cloudiness and mixing height are available. Fortunately, the mixing height and the cloudiness are quite

insignificant because they play an important role only when the macroscale dispersion is of interest.

3) In 1996, the over-predicted values of ambient PM_{10} concentrations mostly occured in June, July and October because the effects of scavenging by rainfall and reduced dust generation from moist feed materials were not taken into account in the simulation.
4) The emission data and the characteristics of PM_{10} such as the size distribution used in the simulation are based on a survey of only a few stone-processing plants, which might not be a good representative of all 48 stone-processing plants in the study area.
5) Finally, it should be pointed out that one major weakness of the present study is the inappropriate assumption of the source type. According to U.S. EPA user's guide of the ISCST3 model, crushed stone processing and stockpiles should be represented as an area source. However, because of the lack of detailed information on most of the 48 plants, the present study has unrealistically assigned an equivalent point source for each stone-processing plant.

In conclusion, it can be seen that reliable input parameters and valid assumptions are indispensable for any modeling task. Mathematical models work well only when their extensive data input requirements are satisfied, which are seldom in the real world. The ISCST3 model selected for this study have features that take into account of the effect of dry deposition and plume depletion. Though there is still significant discrepancy between the actual measurements and simulation results, it is not possible here to investigate and eliminate all of the identified causes in this study. Therefore, it is worth remembering that all major conclusions obtained in this study are subjected to the same constraints inherent in the ISCST3 model and the assumptions used herewith.

5.2 Statistically Generated Meteorological Inputs

A key factor in the success of Monte-Carlo simulation is the generation of statistically appropriate values of the various types of random variables. In the present study, the well-established statistical package, SPSS, is employed as a tool for analyzing, testing and generating values of meteorological variables. Using available subroutines of SPSS package, this section investigates the statistical values of past meteorological data and identify the procedure for generating random values of meteorological variables.

5.2.1 Wind Speed

All past records of the hourly wind speed observed at the PCD monitoring station in Nah Pra Laan from January 1995 to December 2000 were collected. Hourly wind speed data on the same Julian date of those years were statistically analyzed. The appropriate probability distribution function (PDF) and the suitable values of distribution parameters for the hourly wind speed were subsequently identified by means of the Q-Q (Quantile-Quantile) probability plot. The appropriate type of PDF can be determined with the use of the detrended probability plot, which is basically a plot of the deviation of the recorded data from the assumed probability curve. Figure 5.4 shows the examples of the said comparison for various assumed probability plots (e.g. Normal probability plot, Gamma probability plot, Uniform probability plot, and Laplace probability plot) and their corresponding detrended plots. The analyzed data is the hourly average wind speed at 1 A.M. in the month of January from 1995 to 2000. The solid line in the Q-Q plot represents the expected data values for the assumed PDF, while each dot represents an observed value of the wind speed.

According to Figure 5.4 (a) – (d), which shows the sample of comparison of gamma Q-Q probability distribution plot and detrended plot with historical wind speed data at 1:00 A.M.. Apparently, the gamma distribution appears to be the best-fit distribution of the actual records of wind speed collected at 1:00 A.M. over the past 6 years for the month of January. Similarly, for the hourly average wind speed at other hours of the day, it was found that the gamma distribution is still the best representative probability distribution to describe the stochastic nature of the hourly wind speed in the study area. Therefore, the present study generated the random values of the hourly wind speed according to the gamma distribution with its parametric values obtained from SPSS package. Because of the auto-correlated nature of the wind speed, the exponential smoothing technique has been employed to transform uncorrelated gamma random wind speed variable into auto-correlated gamma random variable by using a suitable weighting parameters (α). To determine the proper value of α, 100 sets of random wind speed variable are first generated and then smoothed by using α values of 0.25, 0.5, or 0.75, respectively.

Figure 5.5 illustrates the comparison between the trends of the actual average diurnal wind speed and the average diurnal of 100 independent sets of auto-correlated gamma random wind speed with different α for January 1995 – 2000. The calculated sum of squares of error (SSE) between the actual wind speed and the auto-correlated gamma random wind speed with α = 0.25, 0.50, and 0.75 are found to be 2.67, 1.39, and 2.59, respectively. It can be seen that the α value of 0.5 gives the most statistically suitable results compared with the actual wind speed data observed in the past years.

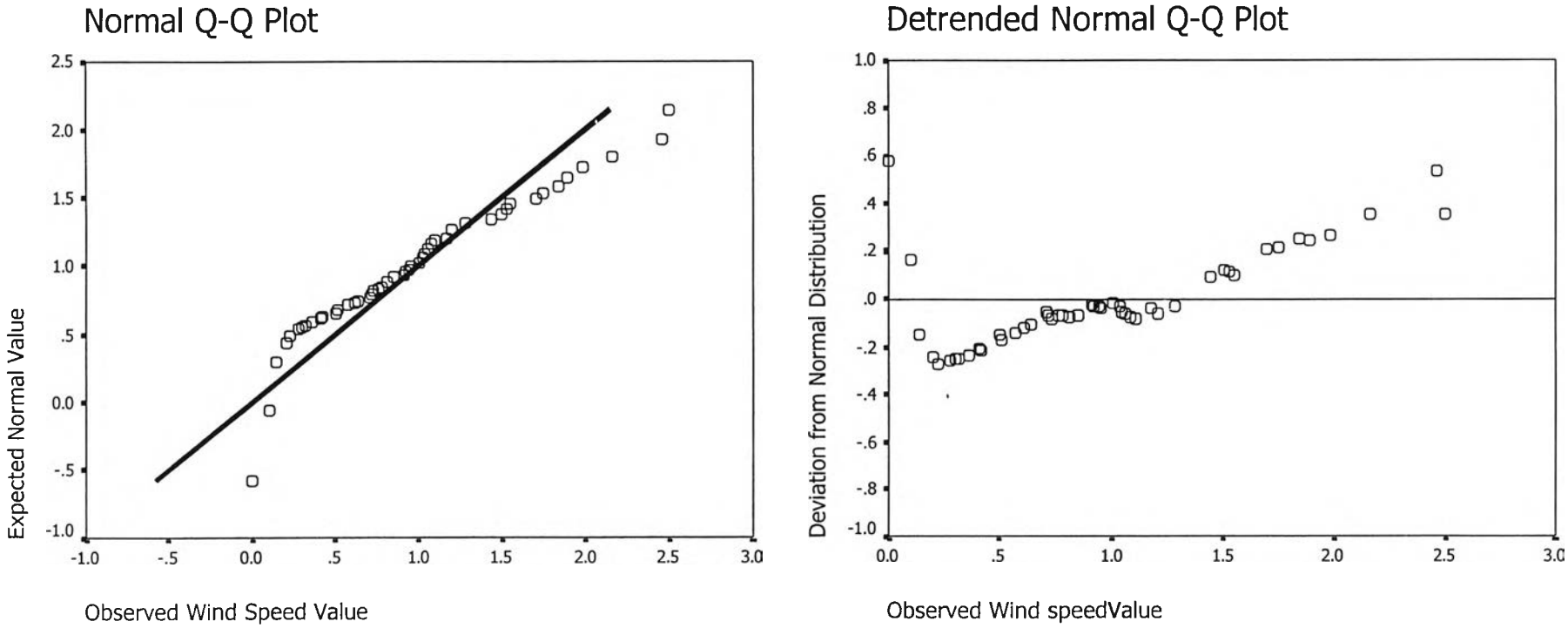

Figure 5.4 **(a)** Comparison of normal Q-Q probability distribution plot and detrended plot with historical wind speed data at 1:00 A.M. for January of 1995 - 2000.

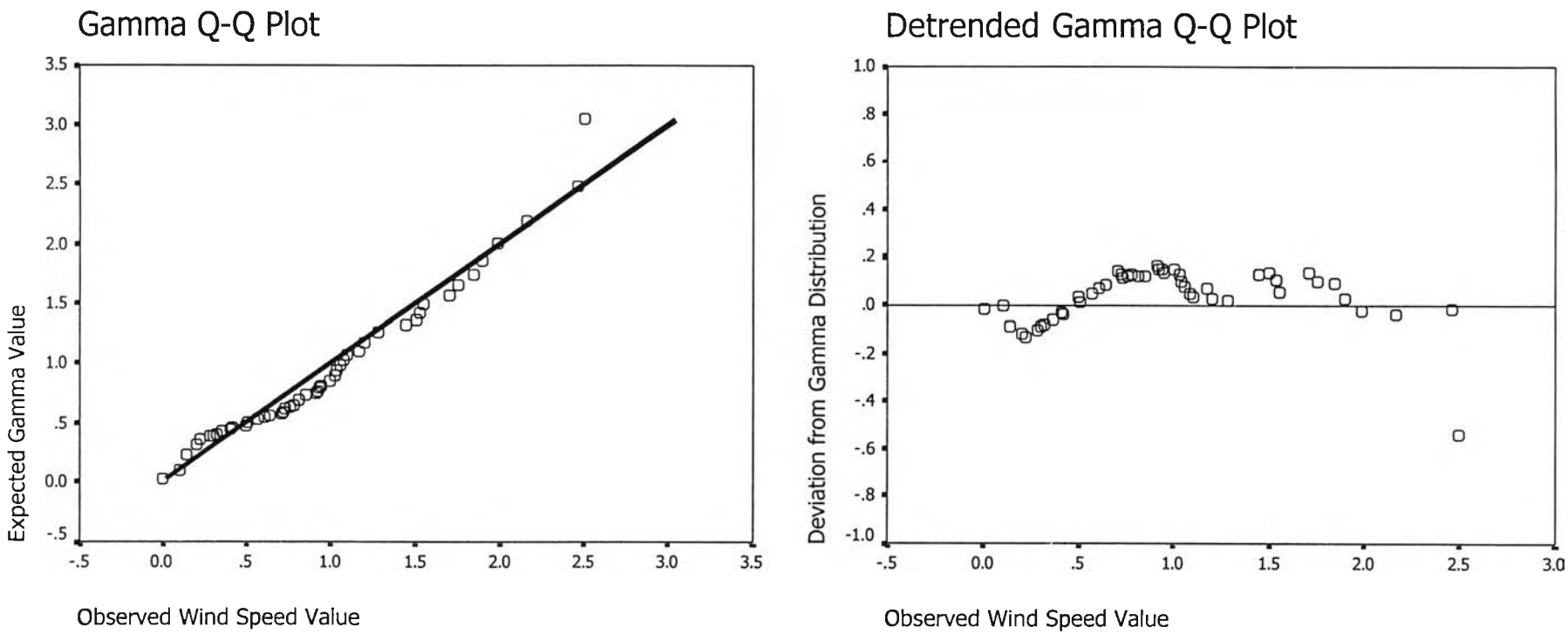

Figure 5.4 (b) Comparison of gamma Q-Q probability distribution plot and detrended plot with historical wind speed data at 1:00 A.M. for January of 1995 – 2000.

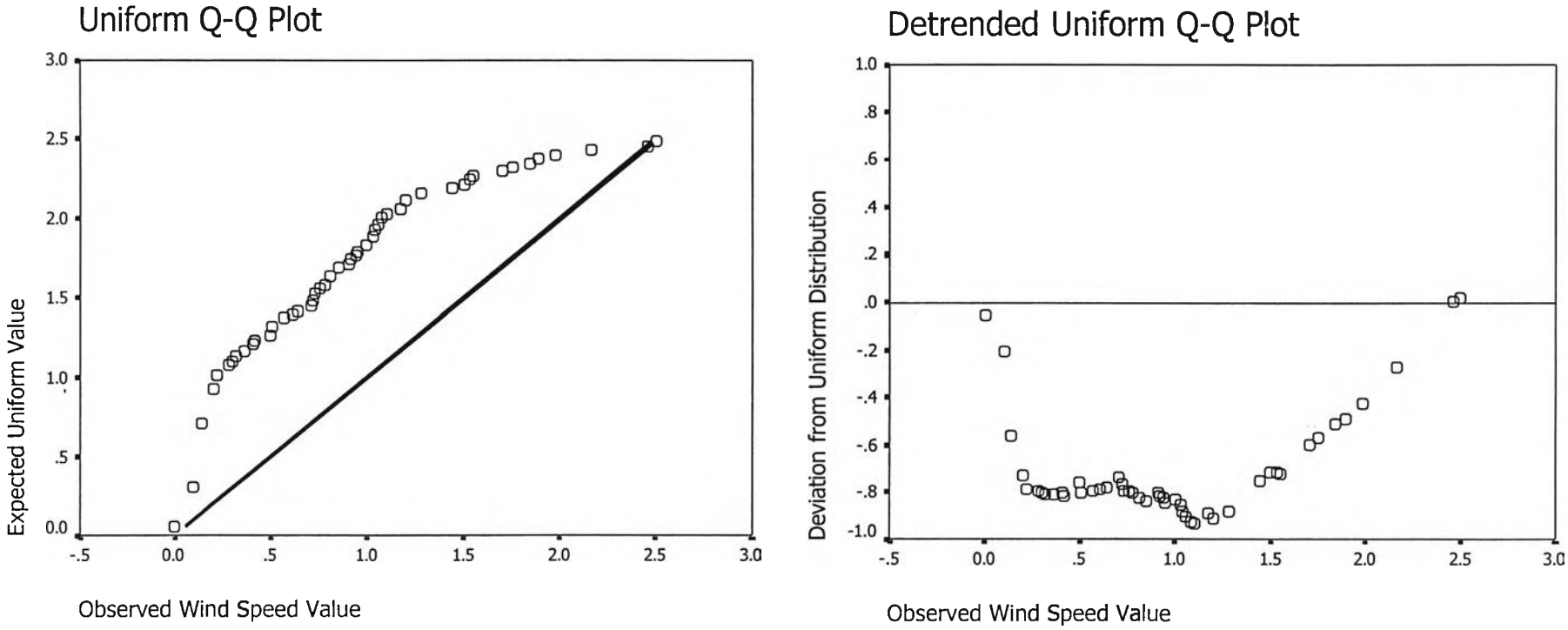

Figure 5.4 (c) Comparison of uniform Q-Q probability distribution plot and detrended plot with historical wind speed data at 1:00 A.M. for January of 1995 - 2000

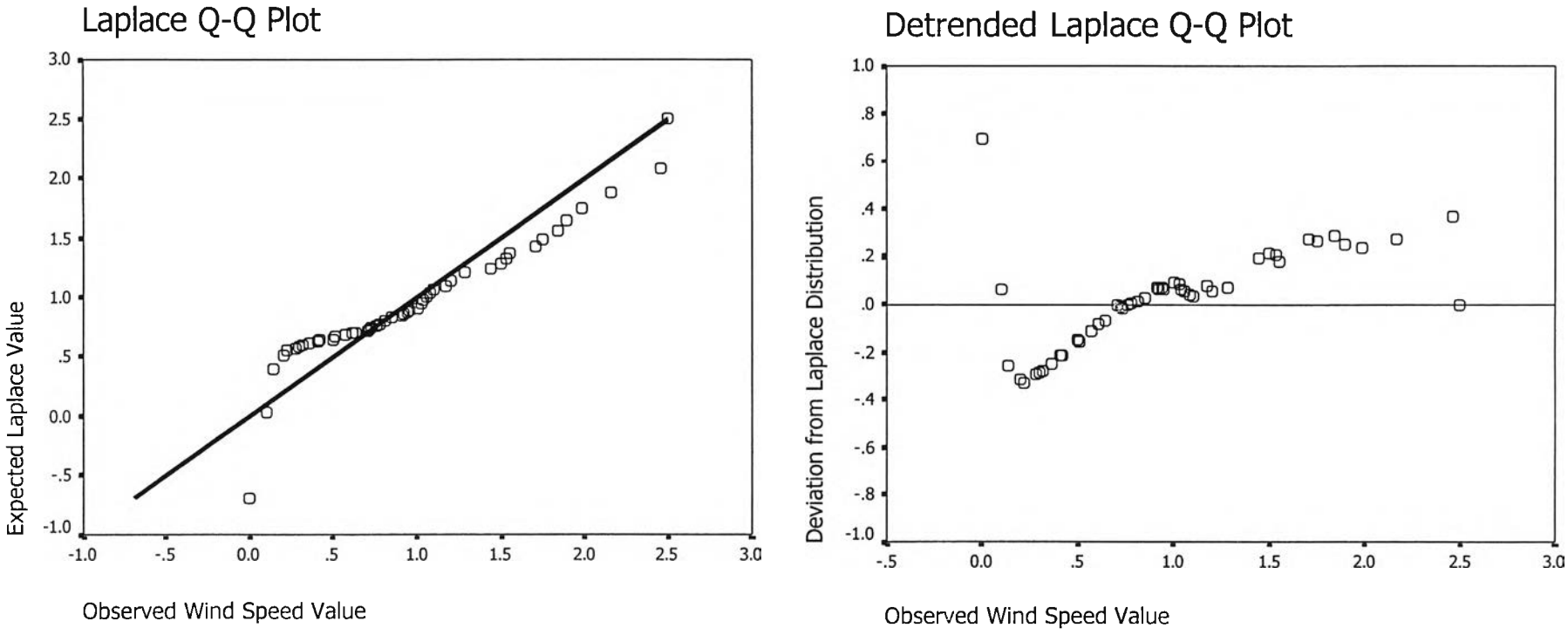

Figure 5.4 (d) Comparison of Laplace Q-Q probability distribution plots and detrended plot with historical wind speed data at 1:00 A.M. for January of 1995 - 2000

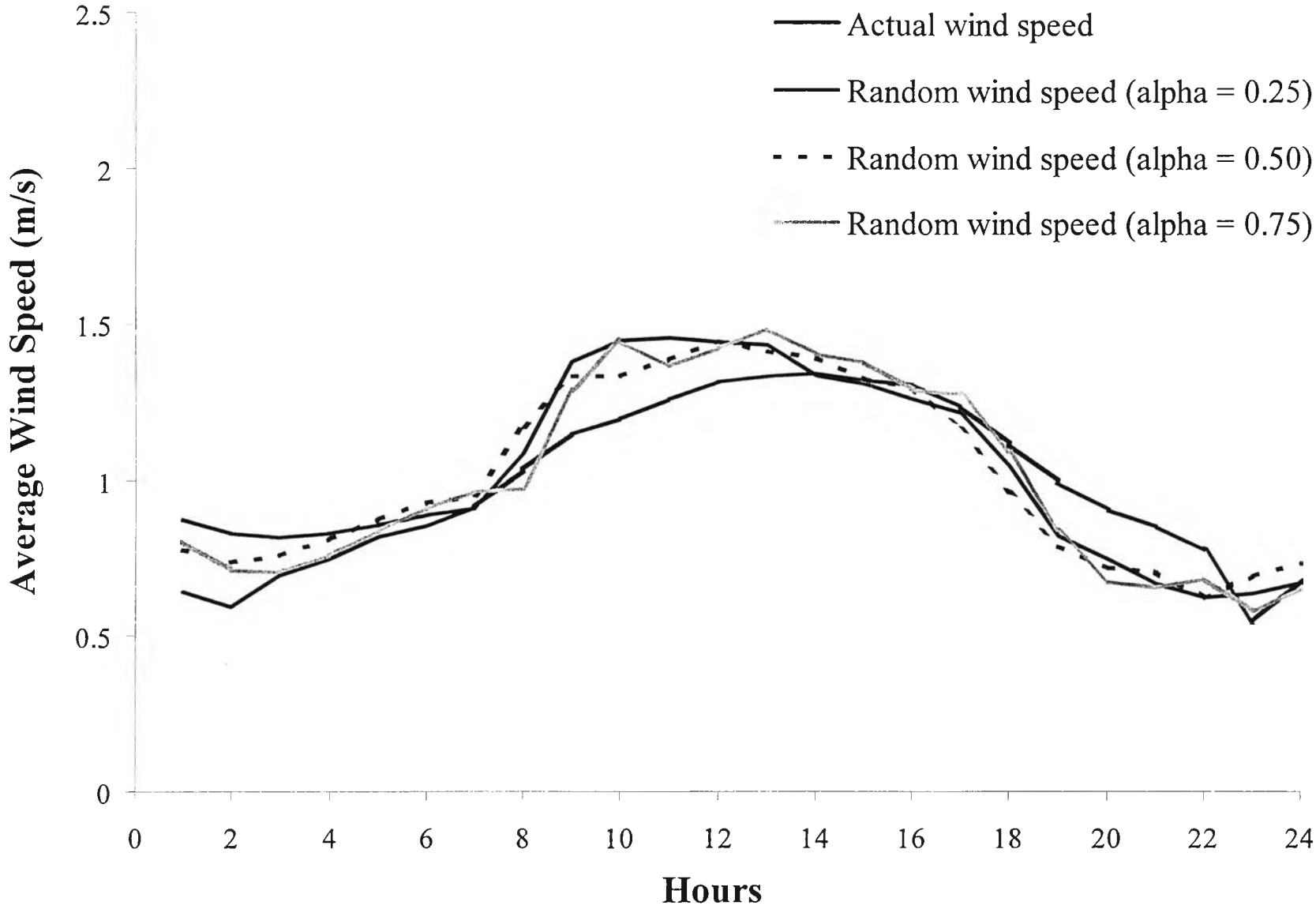

Figure 5.5 Actual average diurnal wind speed *vs.* auto-correlated gamma random wind speed with different weighting parameter (α)

5.2.2 Wind Direction

Historical hourly wind direction data observed in Nah Pra Laan area collected from January 1995 to December 2000 are investigated using the same statistical procedure as the hourly wind speed. Examples of statistical comparison of various probability plots in the case of wind direction at 1 A.M. in January 1995 – 2000 are shown in Appendix C. It can be concluded that the gamma distribution again has the best performance to describe the nature of the actual records of hourly wind direction.

Similarly, for the hourly average wind direction at other hours of the day, it was found that the gamma distribution remains the best representative probability distribution to describe the nature of the hourly wind direction in the study area. Therefore, the present study generated the random values of the hourly wind direction according to the gamma distribution with its parametric values obtained from the SPSS package. Because of the auto-correlated nature of the wind direction, the exponential smoothing technique has been employed to transform uncorrelated gamma random wind direction variable into auto-correlated gamma random variable by using a suitable weighting parameters (α). To determine the proper value of α, 100 sets of random wind direction variable are first generated and then smoothed by using α values of 0.25, 0.5, or 0.75, respectively.

For the proper value of weighting parameter, Figure 5.6 illustrates the comparison between the trends of the actual average diurnal wind direction and the average diurnal of 100 sets of auto-correlated gamma random wind direction with different α for January 1995 – 2000. The calculated sum of squares of error (SSE) between the actual wind direction and the auto-correlated gamma random wind direction with α = 0.25, 0.50, and 0.75 are found to be 209.68, 125.98, and 142.14, respectively. It can be seen that the α value of 0.5 gives the most statistically suitable results compared with the actual wind direction data observed in the past years.

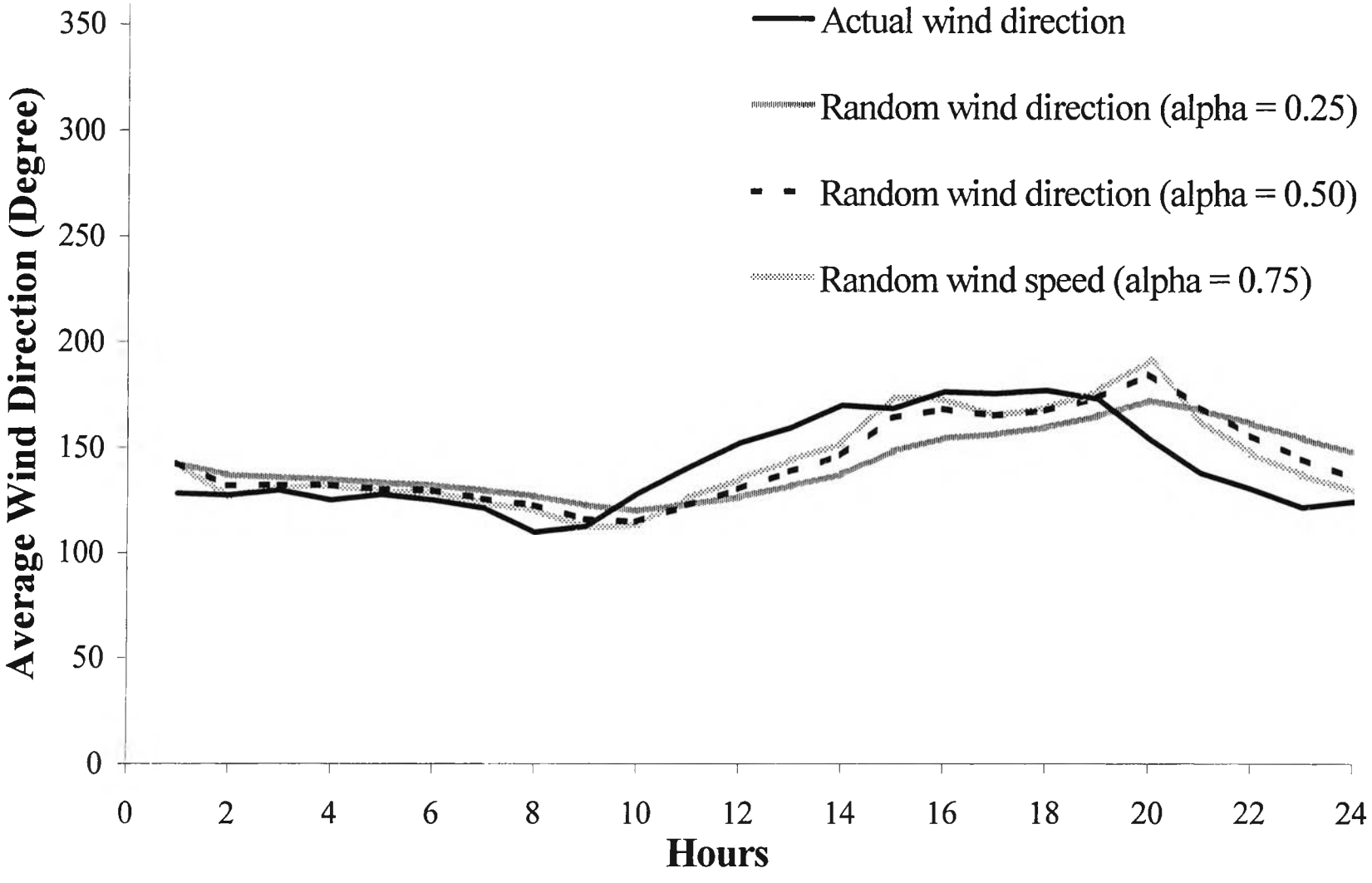

Figure 5.6 Actual average diurnal wind direction *vs.* auto-correlated gamma random wind direction with different weighting parameter (α)

5.2.3 Ambient Temperature

Historical hourly ambient temperature data observed in Nah Pra Laan area collected from January 1995 to December 2000 are investigated using the same statistical procedure as the hourly wind speed. Examples of statistical comparison of various probability plots in the case of ambient temperature at 1 A.M. in January 1995 – 2000 are shown in Appendix C. It can be concluded that the gamma distribution again has the best performance to describe the nature of the actual records of hourly ambient temperature.

Similarly, for the hourly average ambient temperature at other hours of the day, it was found that the gamma distribution remains the best representative probability distribution to describe the nature of the hourly ambient temperature in the study area. Therefore, the present study generated the random values of the hourly ambient temperature according to the gamma distribution with its parametric values obtained from the SPSS package. Because of the auto-correlated nature of the ambient temperature, the exponential smoothing technique has been employed to transform uncorrelated gamma random ambient temperature variable into auto-correlated gamma random variable by using a suitable weighting parameters (α). To determine the proper value of α, 100 sets of random ambient temperature variable are first generated and then smoothed by using α values of 0.25, 0.5, or 0.75, respectively.

For the proper value of weighting parameter, Figure 5.7 illustrates the comparison between the trends of the actual average diurnal ambient temperature and the average diurnal of 100 sets of auto-correlated gamma random ambient temperature with different α for January 1995 – 2000. The calculated sum of squares of error (SSE) between the actual ambient temperature and the auto-correlated gamma random ambient temperature with α = 0.25, 0.50, and 0.75 are found to be 62.40, 24.32, and 28.34, respectively. It can be seen that the α value of 0.5 gives the most statistically suitable results compared with the actual ambient temperature data observed in the past years.

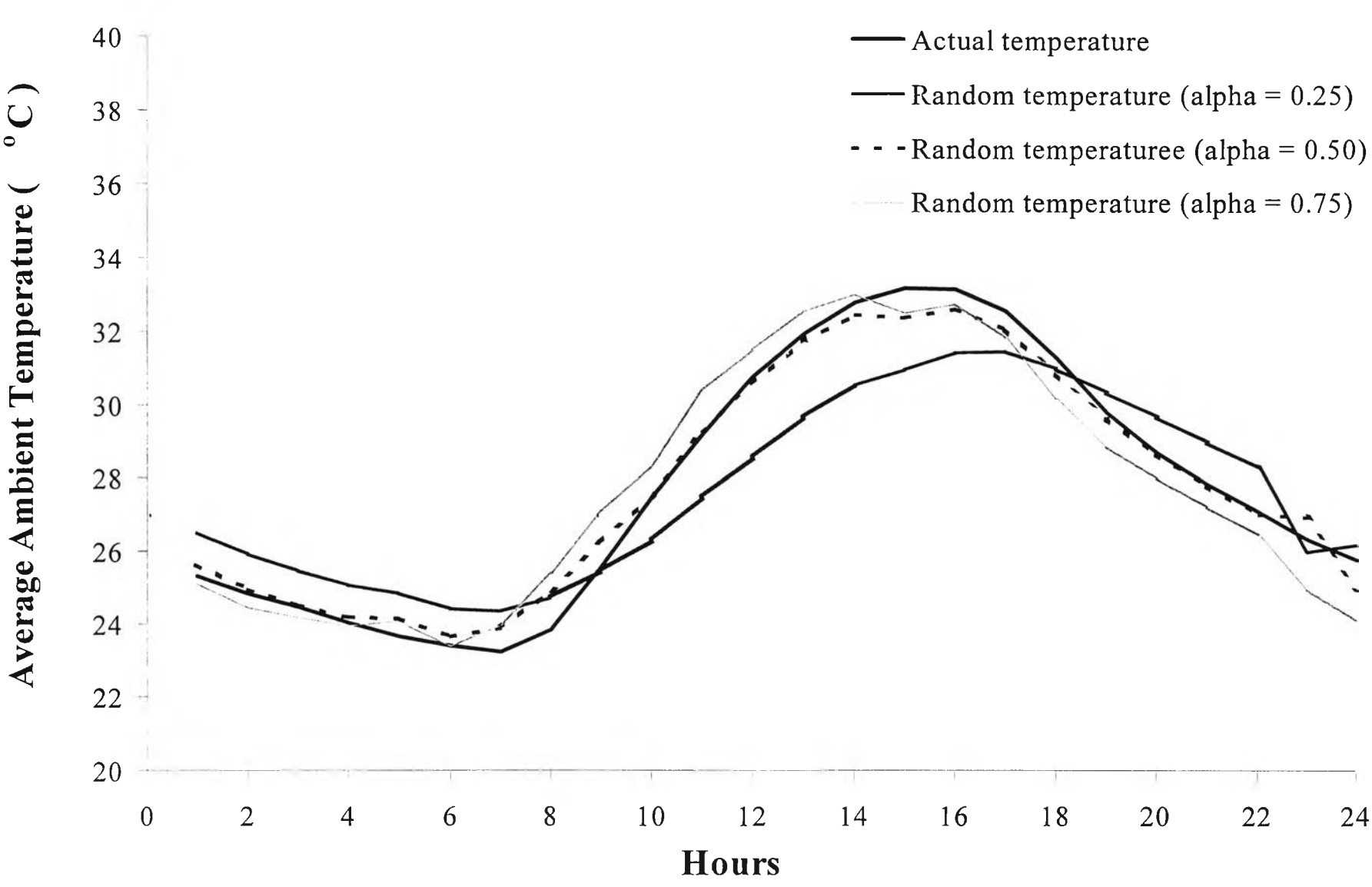

Figure 5.7 Actual average diurnal ambient temperature *vs.* auto-correlated gamma random ambient temperature with different weighting parameter (alpha)

5.2.4 Mixing Height

Historical hourly mixing height data synoptically observed at monitoring station of TMD in Bangkok from January 1993 to December 2000 are investigated using the same statistical procedure as the hourly wind speed. Examples of statistical comparison of various probability plots in the case of mixing height at 1 A.M. in January 1993 – 2000 are shown in Appendix C. It can be concluded that the gamma distribution again has the best performance to describe the nature of the actual records of hourly mixing height.

Similarly, for the hourly average mixing height at other hours of the day, it was found that the gamma distribution remains the best representative probability distribution to describe the nature of the hourly mixing height. Therefore, the present study generated the random values of the hourly mixing height according to the gamma distribution with its parametric values obtained from the SPSS package. Because of the auto-correlated nature of the mixing height, the exponential smoothing technique has been employed to transform uncorrelated gamma random mixing height variable into auto-correlated gamma random variable by using a suitable weighting parameters (α). To determine the proper value of α, 100 sets of random mixing height variable are first generated and then smoothed by using α values of 0.25, 0.5, or 0.75, respectively.

For the proper value of weighting parameter, Figure 5.8 illustrates the comparison between the trends of the actual average diurnal mixing height and the average diurnal of 100 sets of auto-correlated gamma random mixing height with different α for January 1993 – 2000. The calculated sum of squares of error (SSE) between the actual mixing height and the auto-correlated gamma random mixing height with α = 0.25, 0.50, and 0.75 are found to be 5731.28, 5147.57, and 5760.34, respectively. It can be seen that the α value of 0.5 gives the most statistically suitable results compared with the actual mixing height data observed in the past years.

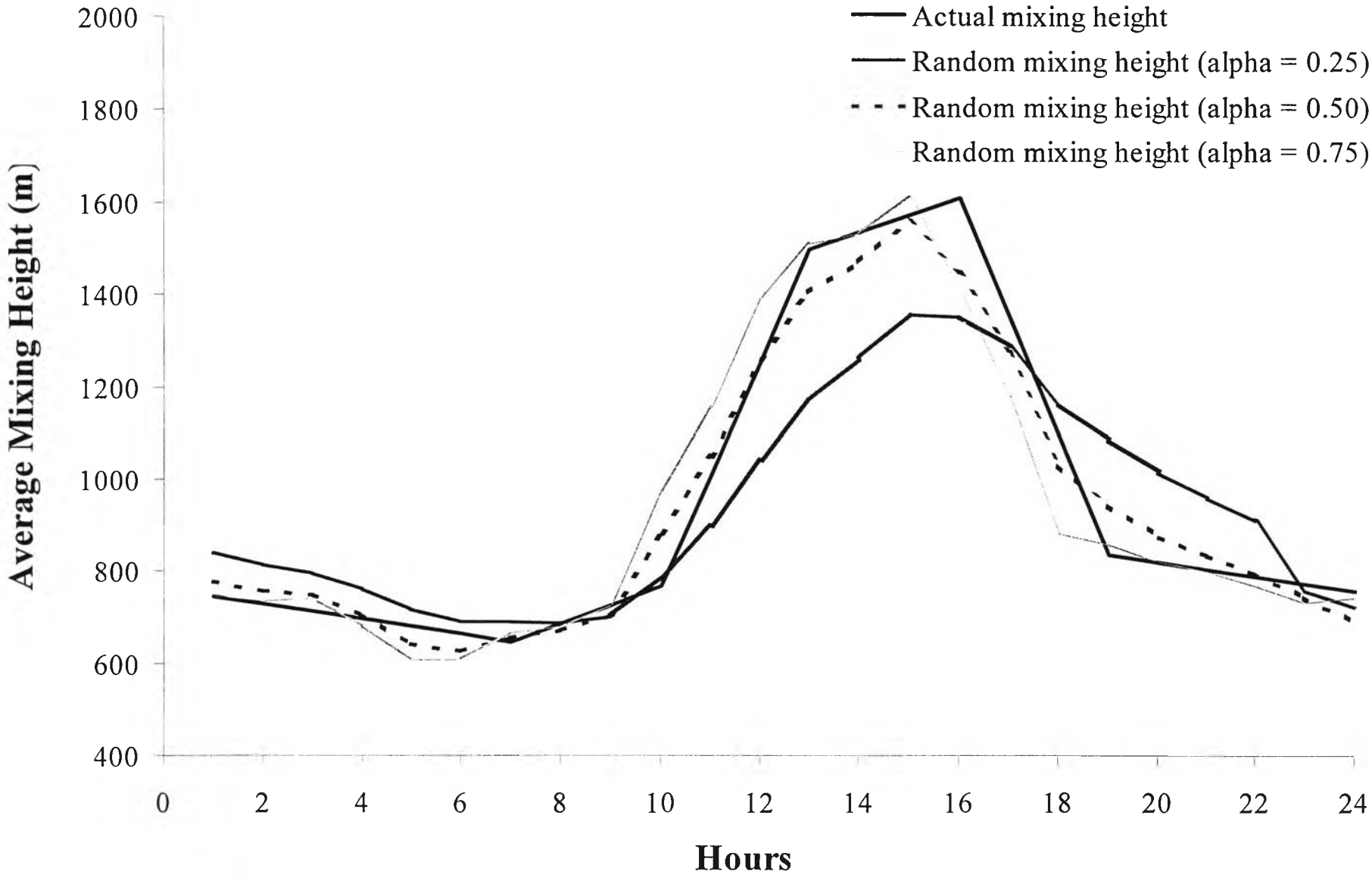

Figure 5.8 Actual average diurnal mixing height *vs.* auto-correlated gamma random mixing height with different weighting parameter (α)

5.2.5 Cloudiness

Historical cloudiness data synoptically observed at monitoring station of TMD in Lopburi from January 1981 to December 2000 are investigated using the same statistical procedure as the hourly wind speed. Examples of statistical comparison of various probability plots in the case of cloudiness at 1 A.M. in January 1981 – 2000 are shown in Appendix C. It can be concluded that the gamma distribution again has the best performance to describe the nature of the actual records of hourly cloudiness.

Similarly, for the hourly average cloudiness at other hours of the day, it was found that the gamma distribution remains the best representative probability distribution to describe the nature of the hourly cloudiness. Therefore, the present study generated the random values of the hourly cloudiness according to the gamma distribution with its parametric values obtained from the SPSS package. Because of the auto-correlated nature of the cloudiness, the exponential smoothing technique has been employed to transform uncorrelated gamma random cloudiness variable into auto-correlated gamma random cloudiness variable by using a suitable weighting parameters (α). To determine the proper value of α, 100 sets of random cloudiness variable are first generated and then smoothed by using α values of 0.25, 0.5, or 0.75, respectively.

For the proper value of weighting parameter, Figure 5.9 illustrates the comparison between the trends of the actual average diurnal cloudiness and the average diurnal of 100 sets of auto-correlated gamma random cloudiness with different α for January 1995 – 2000. The calculated sum of squares of error (SSE) between the actual cloudiness and the auto-correlated gamma random cloudiness with $\alpha = 0.25$, 0.50, and 0.75 are found to be 22.66, 21.65, and 21.97, respectively. It can be seen that the α value of 0.5 gives the most statistically suitable results compared with the actual cloudiness data observed in the past years.

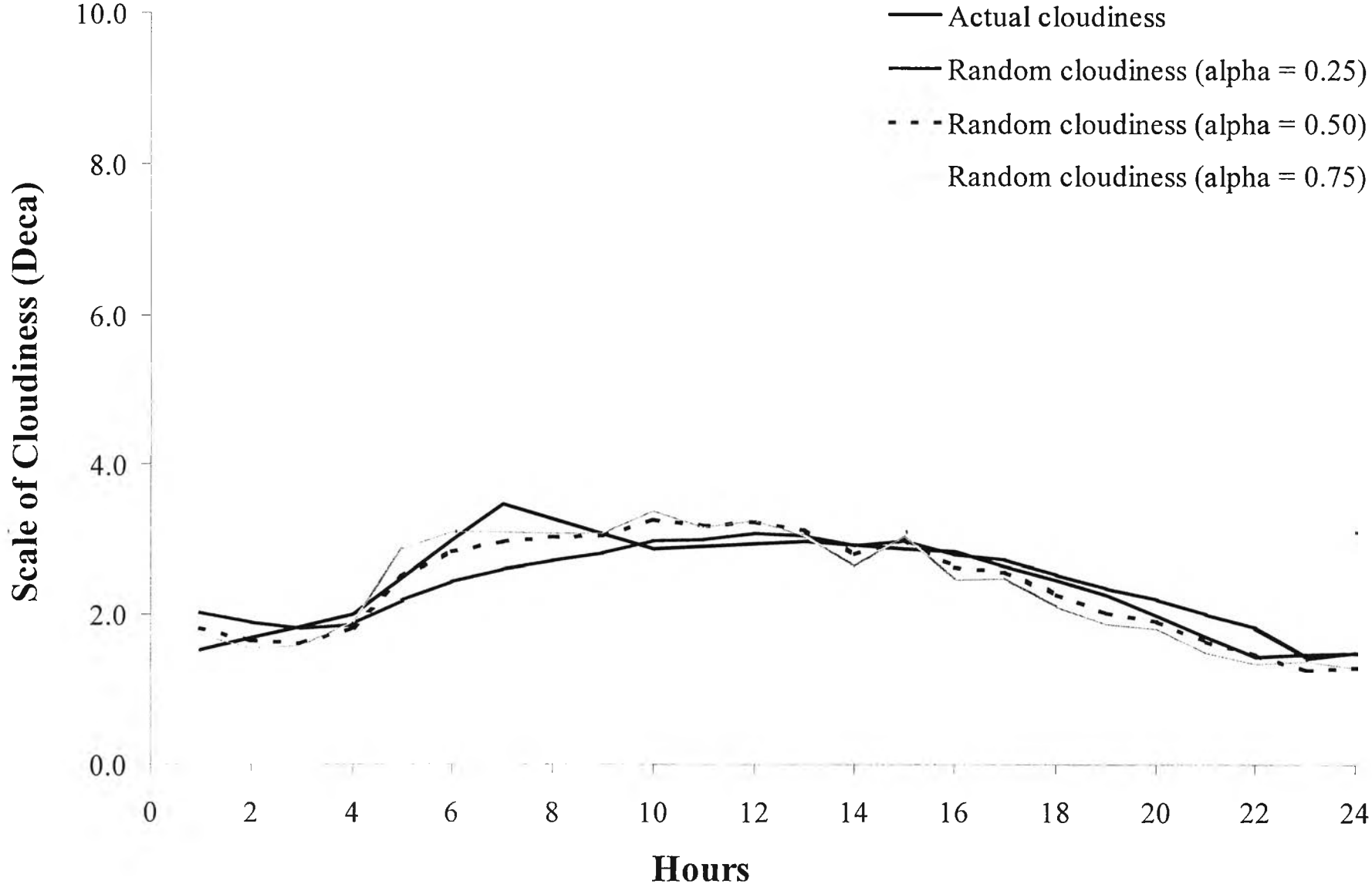

Figure 5.9 Actual average diurnal cloudiness *vs.* auto-correlated gamma random cloudiness with different weighting parameter (α)

5.3 Stochastic Simulation and Analysis of Predicted PM_{10} Concentration

The time-average concentrations of PM_{10} near the ground level were obtained via Monte-Carlo simulations for two different scenarios: the case of uncertain meteorological inputs and the case of uncertain emission rate input. The first scenario examine the effect of uncertainty in the meteorological inputs, perhaps the most important and most difficult to predict, on the uncertainty level in the output PM_{10}concentration.

In this thesis the uncontrolled emission factor, based on the EPA recommended values, is used to estimate the emission rate from the nominal capacity of each stone-processing plant. In reality, no plant is operated at the nominal capacity at all times. In addition, the same type of equipment made by different manufactures may have different uncontrolled emission factors, not to mention the age and maintenance differences. Even if the collection efficiency of the dust suppression system in each plant has the same 80% efficiency, uncertainty in the emission factor still exists. In short, there is always uncertainty in the emission factor used to estimate the emission rate from each of the 48 plants. The second scenario aims to investigate this effect on the output PM_{10} concentration.

This section separately discusses the stochastic analysis of the results obtained from fifty repetitive Monte-Carlo simulations in the case of random meteorological inputs and another fifty simulations set with random emission rate inputs, respectively.

5.3.1 The Case of Random Meteorological Inputs

First, the statistical characteristics of the key meteorological inputs are presented. Figure 5.10 shows the wind rose of the statistically generated hourly wind speed in 16 wind directions throughout all 50 annual sets (438,050 hourly values) of data. The lengths represent respectively the frequencies of occurrence (%) of the three different wind speeds in each direction with respect to the total time. Here the concentric circles represent the scale of frequencies. For example, the wind blew from the south 16 percent of the total time. It blew from the south with wind velocity < 1.5 m/s about 12 % of the time; about 2.5 % of the time it blew from the south with velocities between 1.5 and 2.0 m/s and about 1.5 % of the time it blew from the south with velocity > 2.0 m/s. Note that the direction angle is measured clockwise from the north. The figure reveals that the highest overall probability of wind direction falls in the wind sector of 135^{o} - 180^{o} for wind speeds below 1.5 m/s. In all direction sectors, the wind speed falls in the range of calm wind (0 - 2 m/s) at least 75 % of the total time and is slower than 1.5 m/s at least 50% of the time. The detailed frequency values are shown in Appendix D.

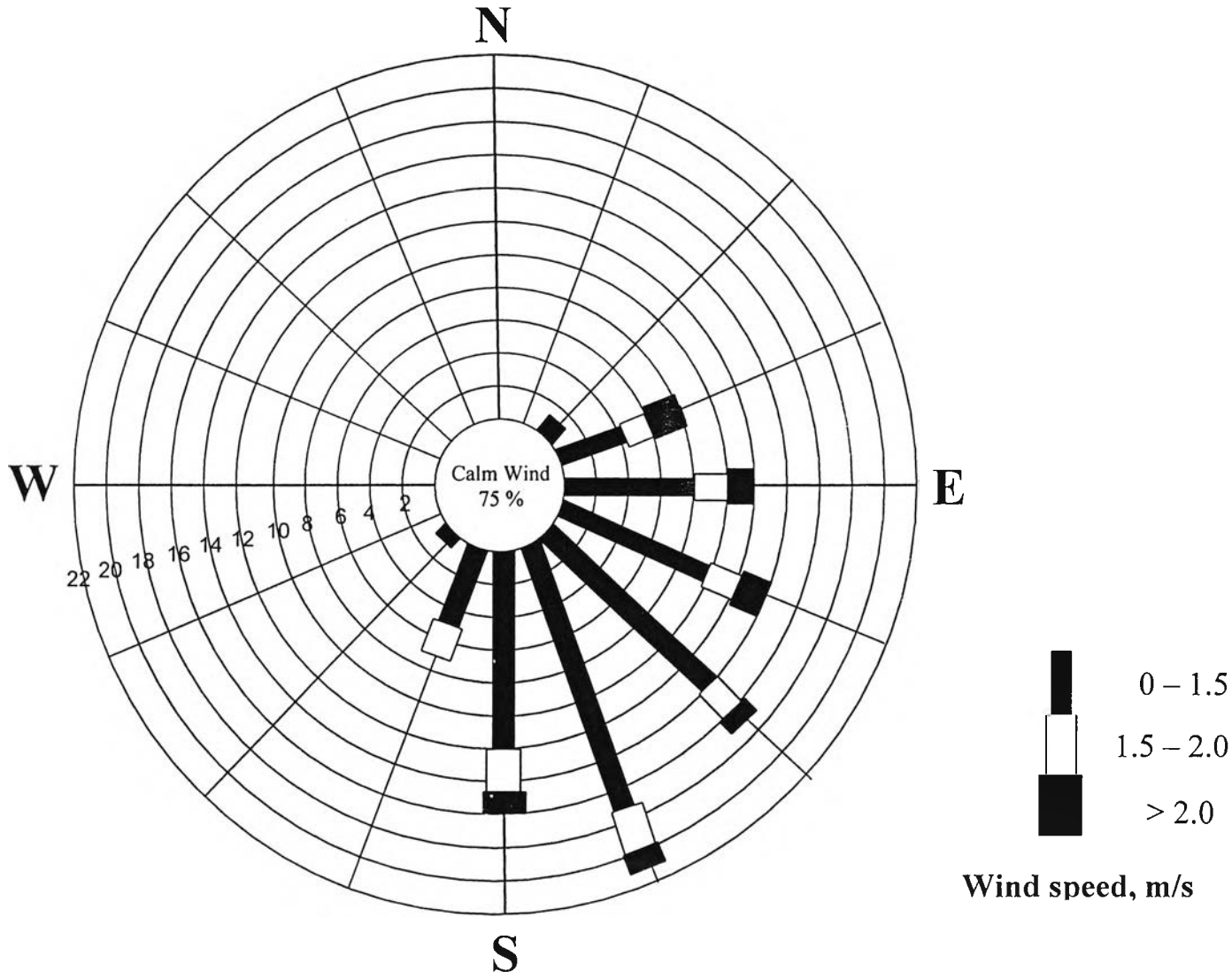

Figure 5.10 Wind rose of the statistically generated hourly wind speed in 16 wind directions throughout all 50 annual sets of data (438,050 hourly values)

To visually grasp the spatial distribution of the stone-processing plants in the whole study region, the location of each plant is presented as a round dot in Figure 5.11, whereas the locations of the five receptors are represented by triangular dots. The shaded area in the figure is the study area of interest.

Figures 5.12 - 5.16 show the various time trends of the 24-hour average PM_{10} predicted at each of the 5 receptors, respectively. Where C 24 is 24-hour average PM_{10} concentrations, C min and C max are the minimum and maximum 24-hour average PM_{10} concentration values, respectively. C 24 + 3SD is 24-hour average PM_{10} concentrations plus 3 times their sample standard deviations.

Referring to the 50-year mean values of the predicted concentration of 24-hour average PM_{10} at each discrete receptor, in Figures 5.12 – 5.16 we see that daily value and the magnitude of annual variation of the 50-year mean of 24-hour PM_{10} at Receptor # 1 is very small compared to that at Receptor # 4, which clearly has much higher mean values on most days and a large variation of the mean values. This is mainly because Receptor # 4 is located downwind of the predominant wind direction, while Receptor # 1 is located upwind of Receptor # 4. In addition, Receptor # 1 is located at an elevated level on the rearside of a high hill which shields it from the PM_{10} emitted by the plants located upwind. In other words, the prevailing southeastern wind plays an important role on the expected (or mean) value of PM_{10} over the northwestern region.

On the other hand, at Receptor # 3 the annual trend of the expected value of the 24-hour PM_{10} appears to be significantly lower from early March to late September than during in the other months of the year. This confirms that the prevailing northeastern wind during the winter (October – February) considerably increases the expected PM_{10} value over the southwestern region.

In Figures 5.12 – 5.16, it is interesting to note that the annual trend of the expected values of the 24-hour average concentration of PM_{10} plus 3 times their sample standard deviation (3SD) are very close to the observed maximum values. One implication is that the statistical distribution of the 24-hour PM_{10} value above the expected (mean) value on the same Julian day at each Receptor point may be approximated as normal (Gaussian) distribution. If this postulate is shown to be valid, then the probability of the future PM_{10} concentration exceeding a certain value on a given day may be estimated from the corresponding Figure.

By the way, a large sample standard deviation of the PM_{10} means that the level of uncertainty in the PM_{10} output is higher. From Figures 5.12 – 5.16, it may be concluded as follows:

1) The higher the expected or mean value of the PM_{10}, the higher the level of uncertainty in its expected value.
2) The magnitude of daily fluctuation in the expected value of the PM_{10} is generally much smaller than that of the daily maximum or the daily sample standard deviation. The reason may be attributed to the interactions between the stochastic or random inputs (wind speed, wind direction, etc.) used in the simulations.

3) The location of a receptor or monitoring station must be made with care and based upon preliminary investigation or simulation results. If possible, as many receptors as feasible should be considered in the selection process. For example, Figure 5.12 reveals that the probability of the 24-hour PM_{10} exceeding the ambient standard concentration value regulated by PCD (120 μ g/m^3) is essentially nil at Receptor # 5 throughout the year. So is the probability at Receptor # 5 except the months of August and September, during which the probability of exceedance is extremely low, though not zero. On the contrary, at Receptor # 4 the probability of exceedance would be higher than 50% of the whole year even after the implementation of dust suppression systems to reduce the emission rate of each plant by 80%. The conclusion is easily reached by looking at the expected (mean) value of the PM_{10} at Receptor # 4. In fact, the detailed simulation results show that the ambient standard concentration value is exceeded on 9,315 days out of the total of 18,250 days.
4) To effectively further reduce the PM_{10} value at Receptor # 4 an across-the-board should not be adopted. Instead it is wise to identify the few plants that contribute heavily to the PM_{10} at Receptor # 4 and target them in the reduction efforts.
5) To reduce the magnitude of uncertainty in the output variable (PM_{10} in this case), it is necessary to minimize the inherent uncertainty in the model inputs and parameters. However, this may be impossible for certain types of inputs such as future meteorological inputs. In addition, there is a saying that "history always repeats itself". In other words, past meteorological records are the best available indicates of the future unless there occurs some unexpected cataclysmic change. This maybe the

main reason that all environmental impact assessment (EIA) studies exclusively rely on historical and current meteorological data. In fact, if there be enough past records, say, over the last 50 years, each set of annual records should be used as inputs in the Monte-Carlo simulation in order to obtain the stochastic nature of the output variables of interest. Because of the lack of such data, the present study has to resort to the use of statistically generated meteorological data.

6) Even if it is impossible to predict future meteorological data, the present stochastic approach is a rational method to estimate the magnitude of uncertainty in the inputs of interest. Once this kind of information on the stochastic characteristics of the outputs is known, it may be used to decide the design margin of the environmental protection system to be installed. In other words, the larger the uncertainty value, the bigger the design margin should be.

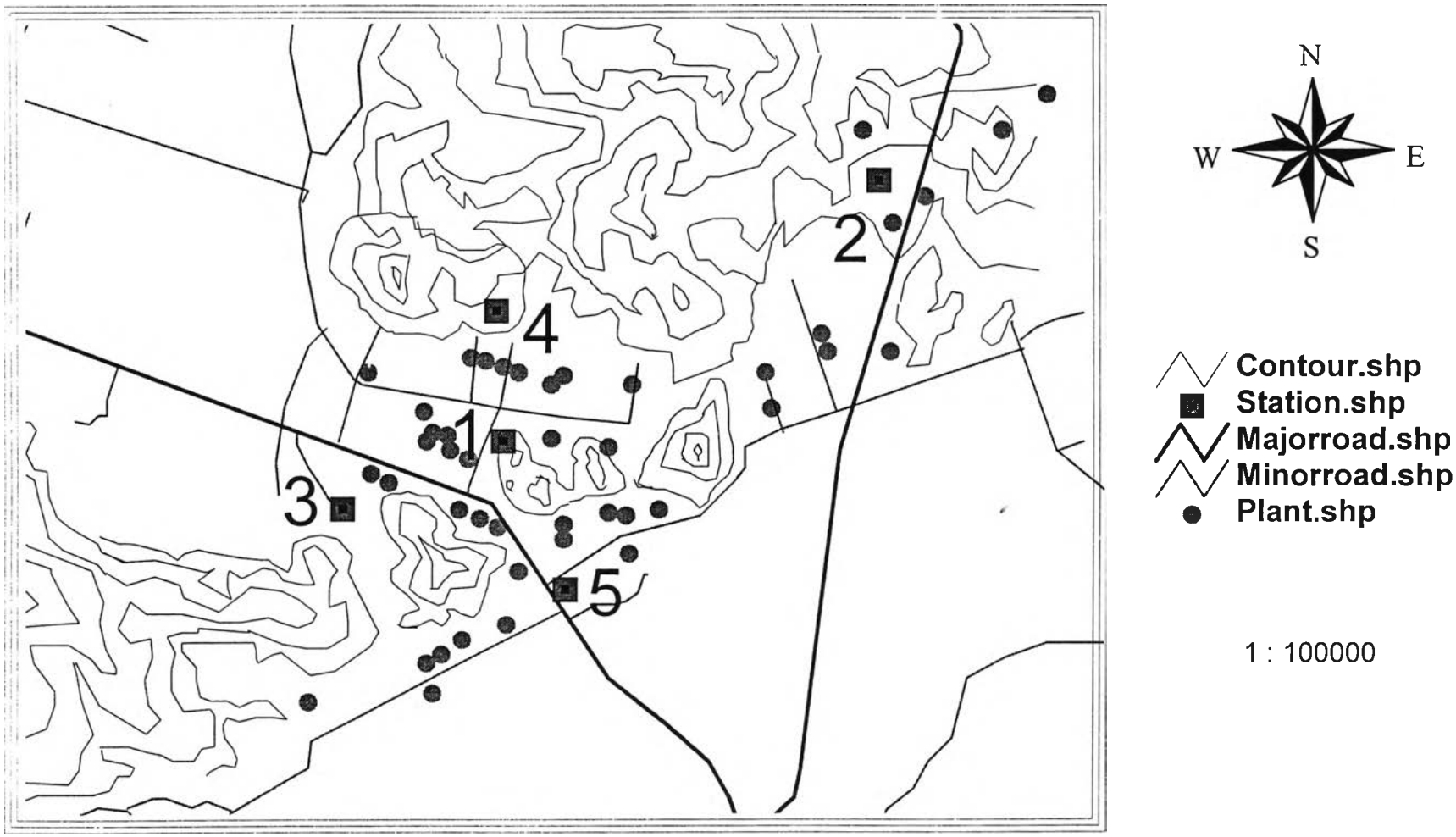

Figure 5.11 Map of study area with locations of stone-processing plants (round dots) and receptors (triangular dots)

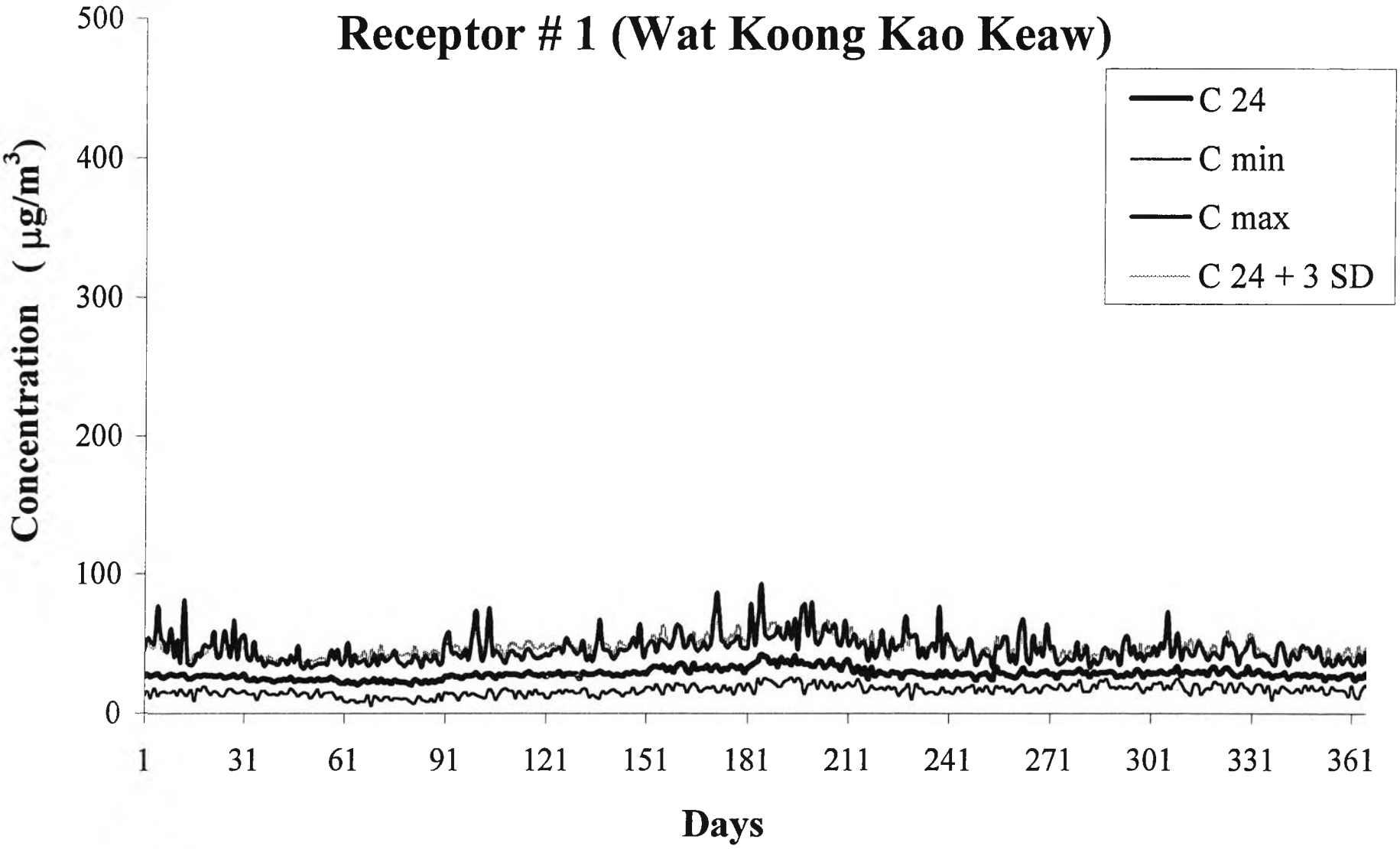

Figure 5.12 Annual trend of the statistical values of 24-hour average concentration of PM_{10} at Wat Koong Kao Keaw obtained from modeling with uncertain meteorological inputs

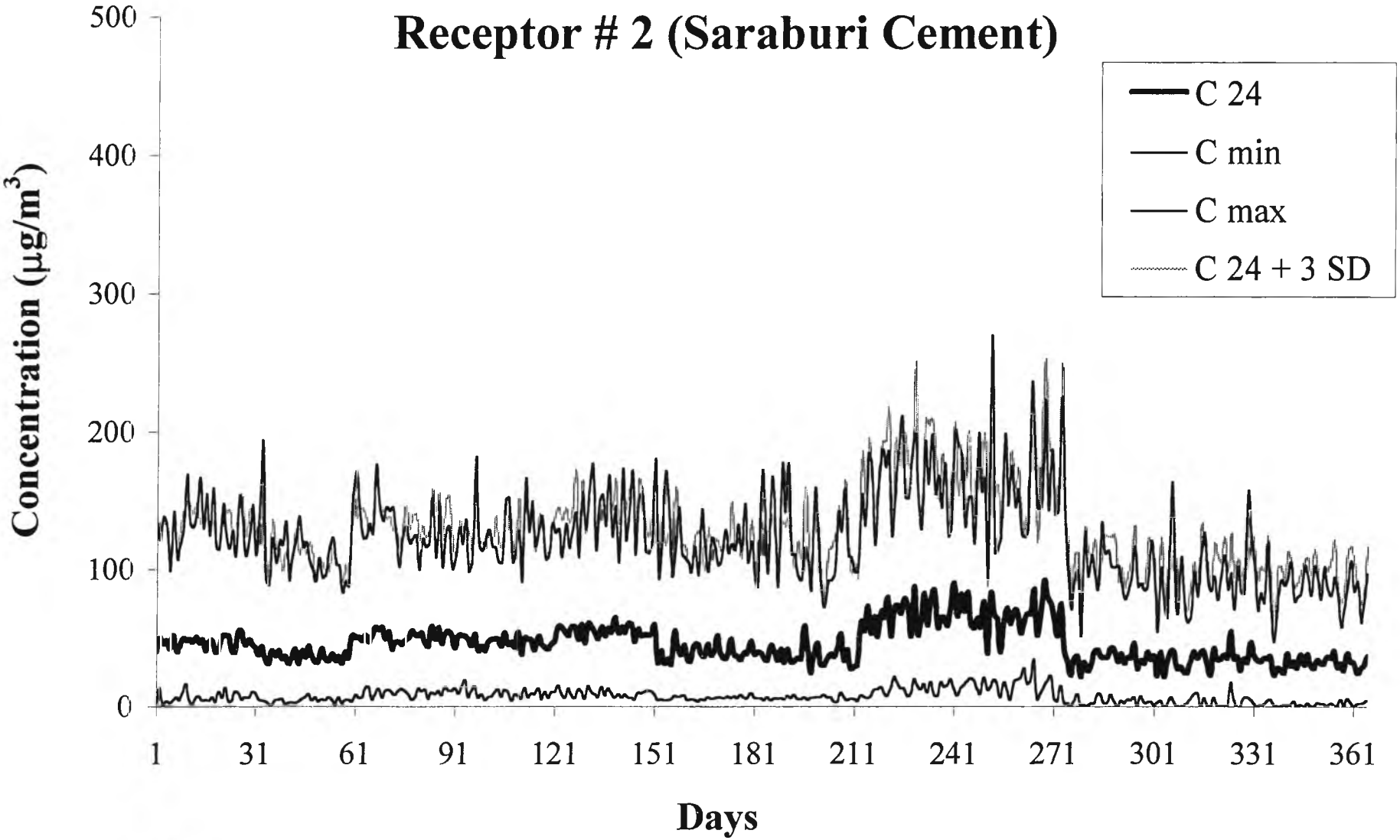

Figure 5.13 Annual trend of the statistical values of 24-hour average concentration of PM_{10} at Saraburi Cement obtained from modeling with uncertain meteorological inputs

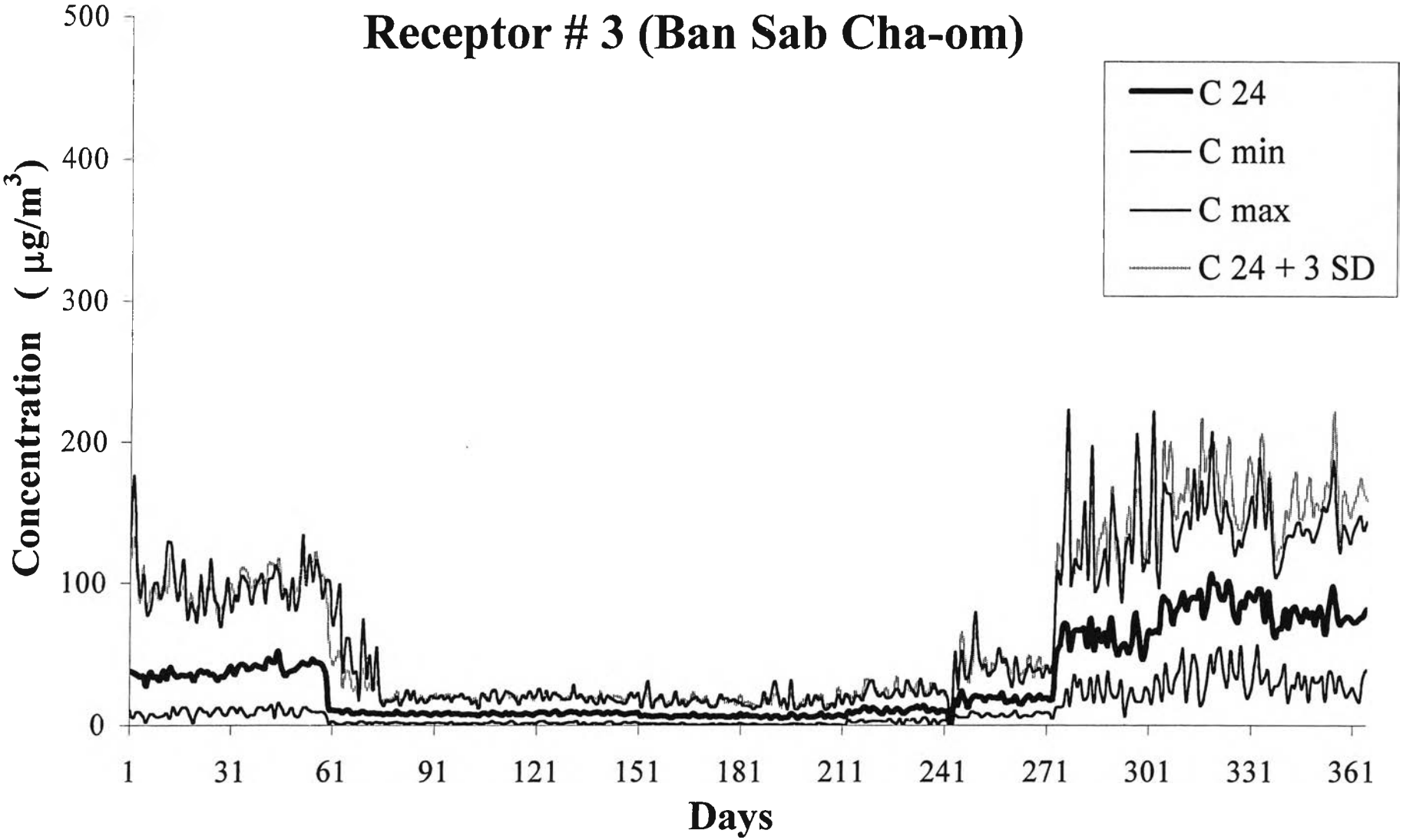

Figure 5.14 Annual trend of the statistical values of 24-hour average concentration of PM_{10} at Ban Sab Cha-om obtained from modeling with uncertain meteorological inputs

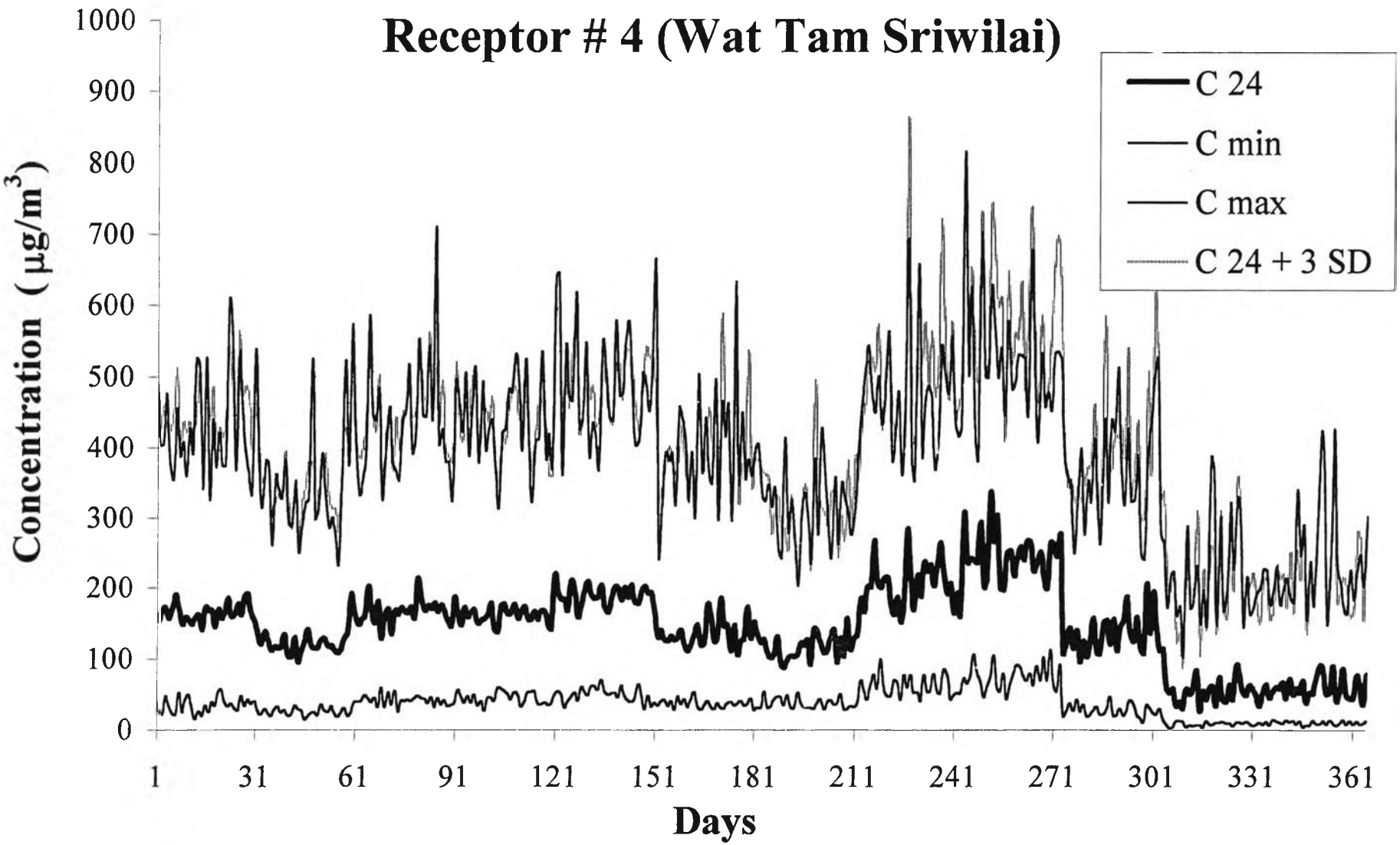

Figure 5.15 Annual trend of the statistical values of 24-hour average concentration of PM_{10} at Wat Tam Sriwilai obtained from modeling with uncertain meteorological inputs

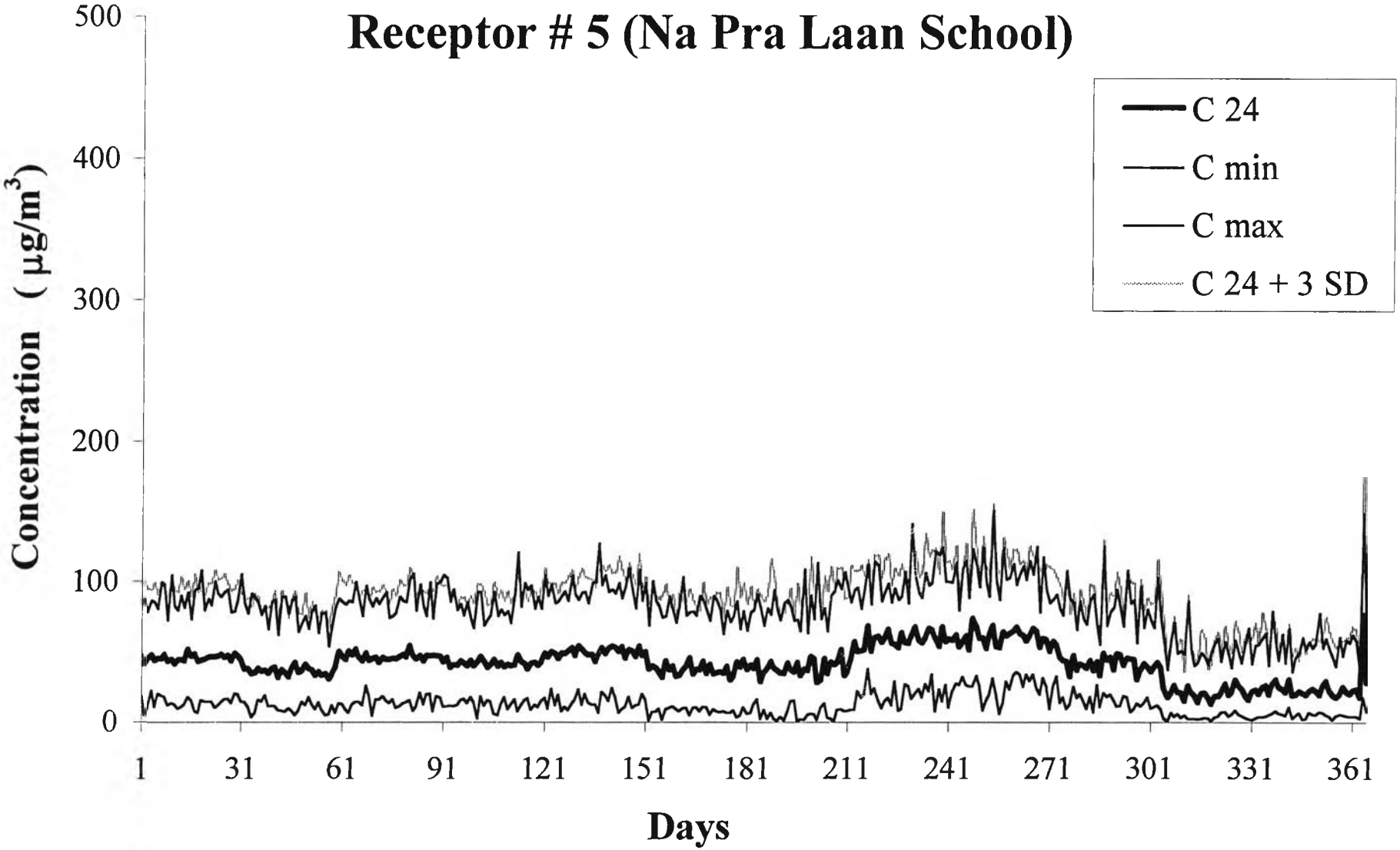

Figure 5.16 Annual trend of the statistical values of 24-hour average concentration of PM_{10} at Na Pra Laan School obtained from modeling with uncertain meteorological inputs

5.3.2 The Case of Random Emission Inputs

Because of lack of measurement data on the emission rate of each piece of equipment in the 48 stone-processing plants of interest, it is necessary to rely on the emission factor provided by U.S. EPA for stone processing to estimate the emission rate inputs to the simulation model. Since the actual production capacity generally depends on the market demand and only the nominal plant capacity registered with the Department of Industrial Works, Ministry of Industry, is known for each plant, the plant emission rate (PM_{10} input) has to be estimated from the available uncertain information. The details in calculating the emission rate of each stone-crushing plant are described in Appendix B.

The present section investigates the effect of the uncertainty in the emission rate inputs on the output PM_{10}. To quantify the magnitude of uncertainty in the emission inputs, it was assumed here that the emission factors can be characterized as random normal variables, whereas the nominal plant capacities are assumed unchanged. Values of the normal random emission factors are generated using the specified mean and standard deviation of the normal distribution. The mean value of the emission factor used in this study is 0.05275 kg/ton, while the standard deviation is assumed to be 10% of the mean, which is 0.005275. Next fifty sets of random emission rates were generated and Monte-Carlo simulation was carried out to determine the trend and statistical properties of the 24-hour average PM_{10}. As for the meteorological inputs used in this case, the hourly data obtained by averaging over the same fifty annual sets of meteorological inputs used in the previous section were calculated and used as inputs to each of the fifty repetitive simulations.

Figures 5.17 – 5.21 show the time trends of the various 24-hour average PM_{10} predicted at each of the 5 receptors, respectively. As discussed before, Receptor # 1 has small expected values of the 24-hour average concentration because of its location and prevailing wind direction. For similar reasons, the expected values of the 24-hour average concentration at Receptor # 3 increase significantly during the winter months (October – December). However, expected values at both receptors rarely exceed the ambient standard concentration value of 120 $\mu g/m^3$.

At Receptor # 4, large expected values are seen in the annual trend of the 24-hour average concentration during August – September because of the high frequency of southwest wind direction and because several stone-crushing plants are located upwind. From Figures 5.17 – 5.21, it is evident that the expected or mean values plus 3 times their sample standard deviations (3SD) are very close to the observed maximum values.

By the way, the probability of the 24-hour average PM_{10} value exceeding the ambient standard concentration value are not negligibly small at Receptor # 2, # 3, # 4, and # 5. Particularly at Receptor # 4, the probability of ambient standard concentration exceedance is about 45% of the overall 50 annual runs (164 days on an annual basis). However, the probability is essentially nil at Receptor # 1. This is because the location of a receptor and the prevailing meteorological data have a remarkable impact on the modeled concentration and its trend. Even after an 80% reduction of plant emission rates is implemented, occasional instances of ambient standard concentration exceedance can be expected at certain times and points.

It is interesting to compare the cases of random meteorological inputs (Figures 5.12 – 5.16) and random emission rate inputs (Figure 5.17 – 5.21). Obviously, the magnitude of uncertainty in the 24-hour PM_{10} in the latter case is very small despite a relatively large standard deviation of 10%. Therefore, it may be concluded that uncertainty in the meteorological inputs has more significant effect on PM_{10} uncertainty than that in the emission rate inputs. On the contrary, uncertainty or variation in the emission inputs has strong direct impact on the expected or mean value of PM_{10}. This leads to sharper fluctuation in the expected values of PM_{10} at those receptors that are located downwind. Since the same set of meteorological data is used as inputs to all 50 simulations in the case of random emission inputs, the emission rate inputs are expected to directly and proportionally affect the expected values of PM_{10}.

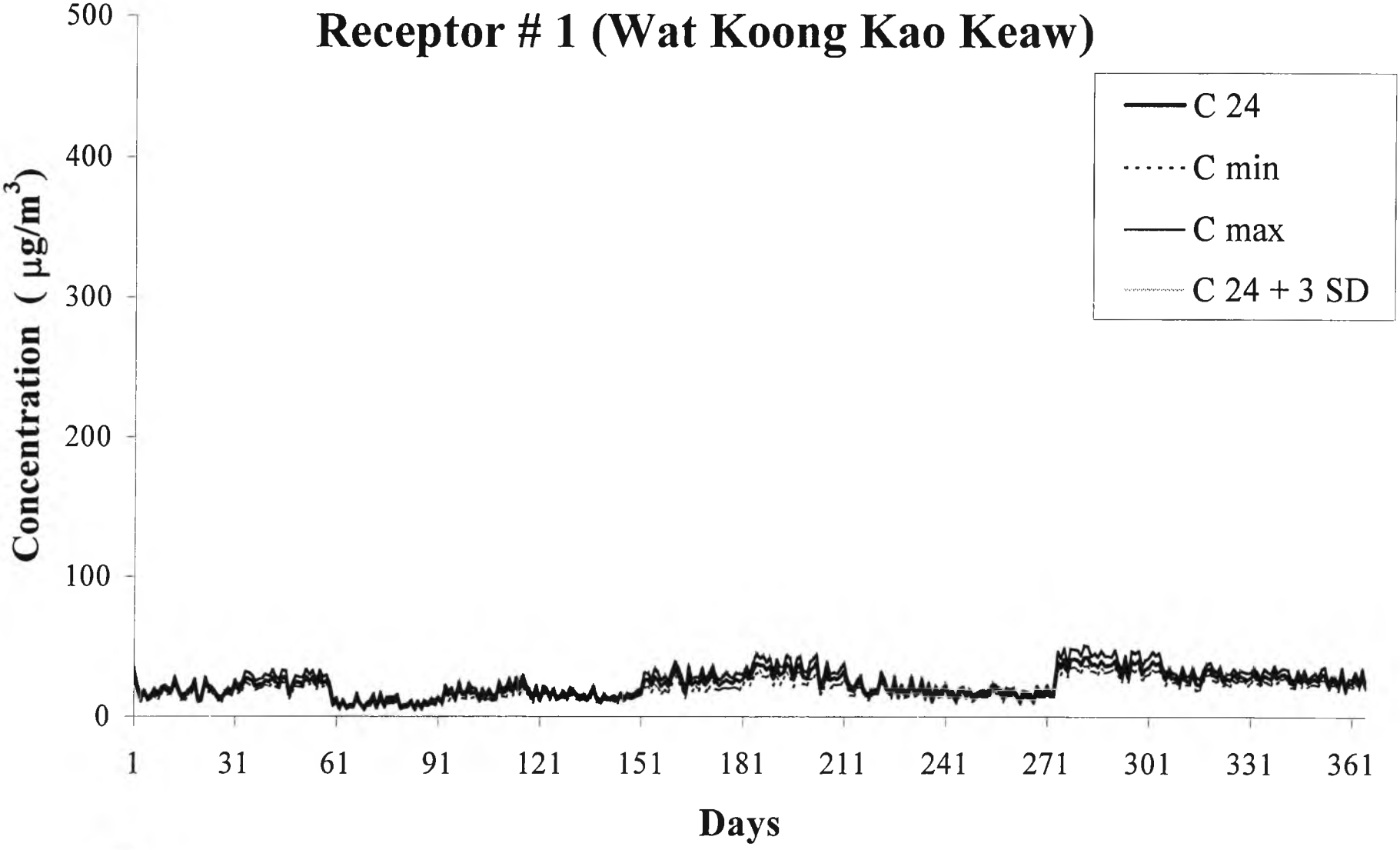

Figure 5.17 Annual trend of the statistical values of 24-hour average concentration of PM_{10} at Wat Koong Kao Keaw obtained from modeling with uncertain emission input

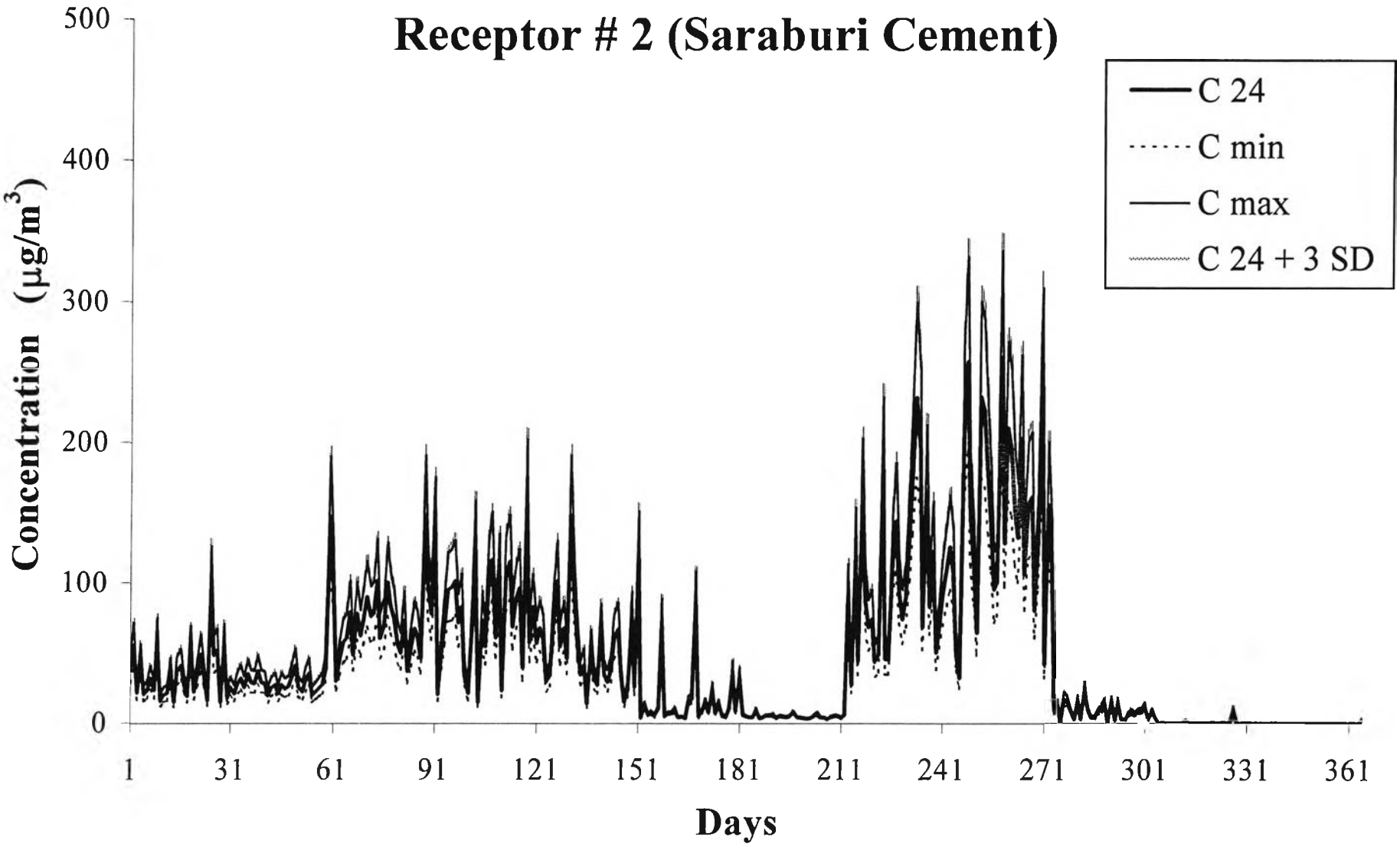

Figure 5.18 Annual trend of the statistical values of 24-hour average concentration of PM_{10} at Saraburi Cement obtained from modeling with uncertain emission input

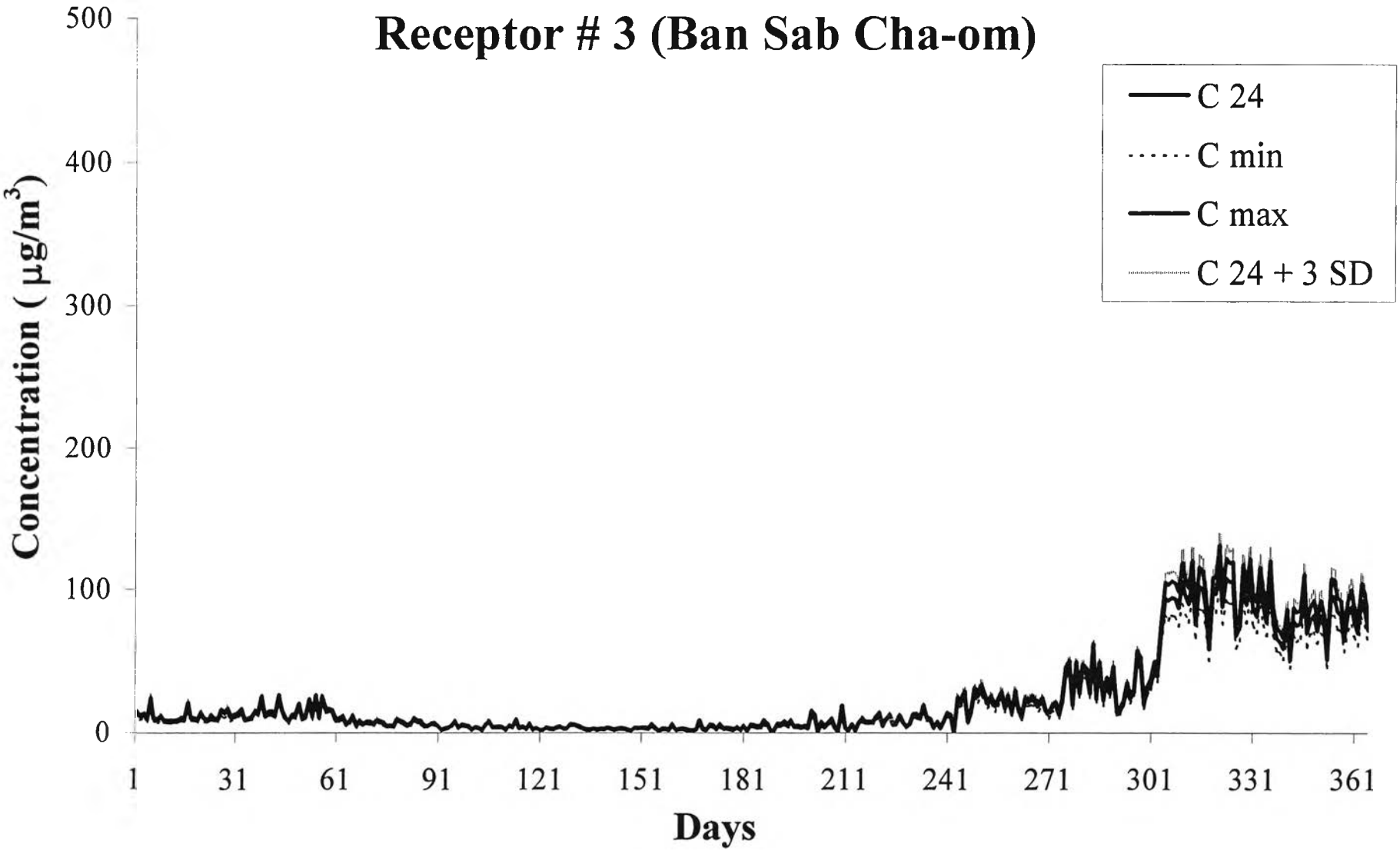

Figure 5.19 Annual trend of the statistical values of 24-hour average concentration of PM_{10} at Ban Sab Cha-om obtained from modeling with uncertain emission input

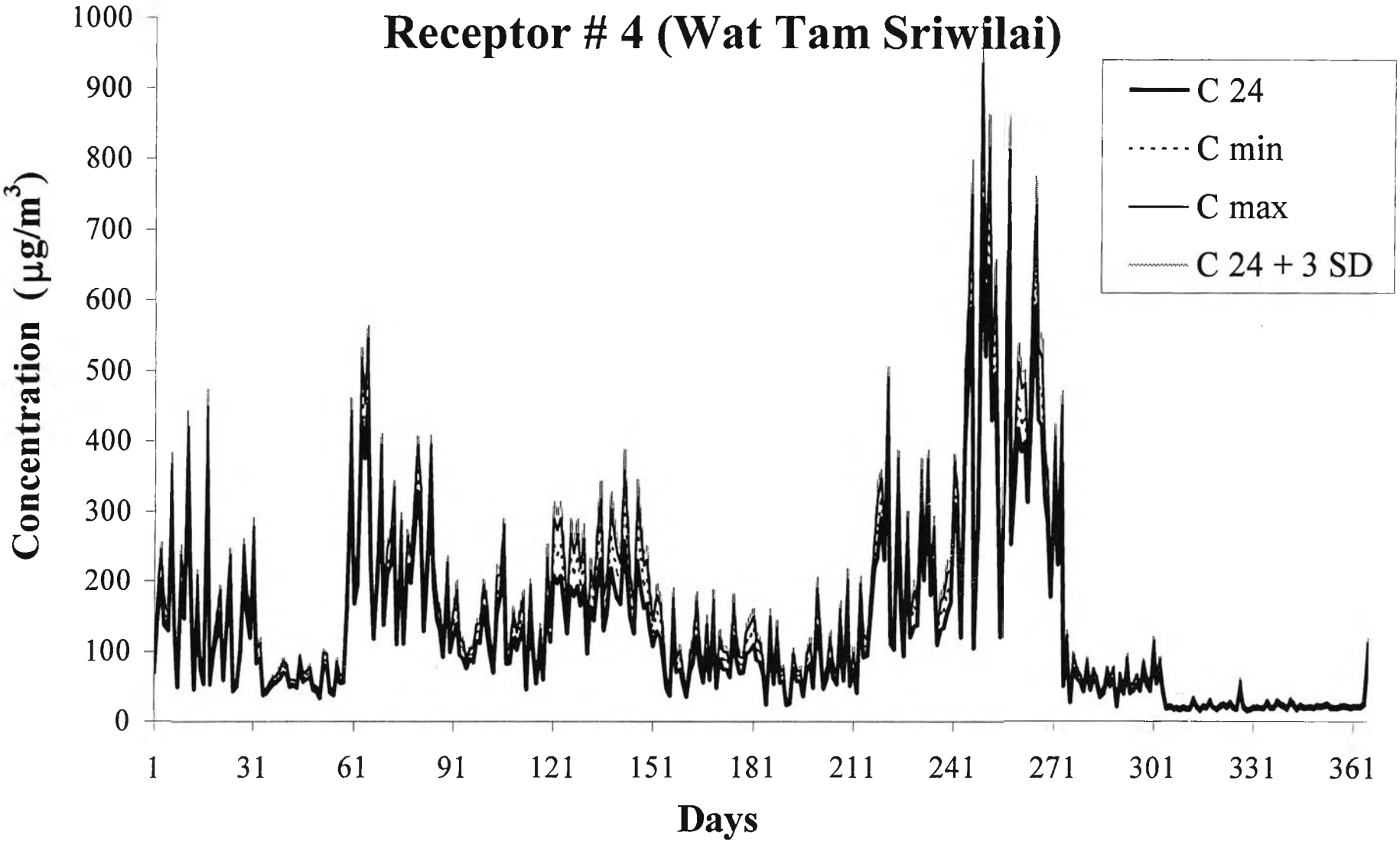

Figure 5.20 Annual trend of the statistical values of 24-hour average concentration of PM_{10} at Wat Tam Sriwilai obtained from modeling with uncertain emission input

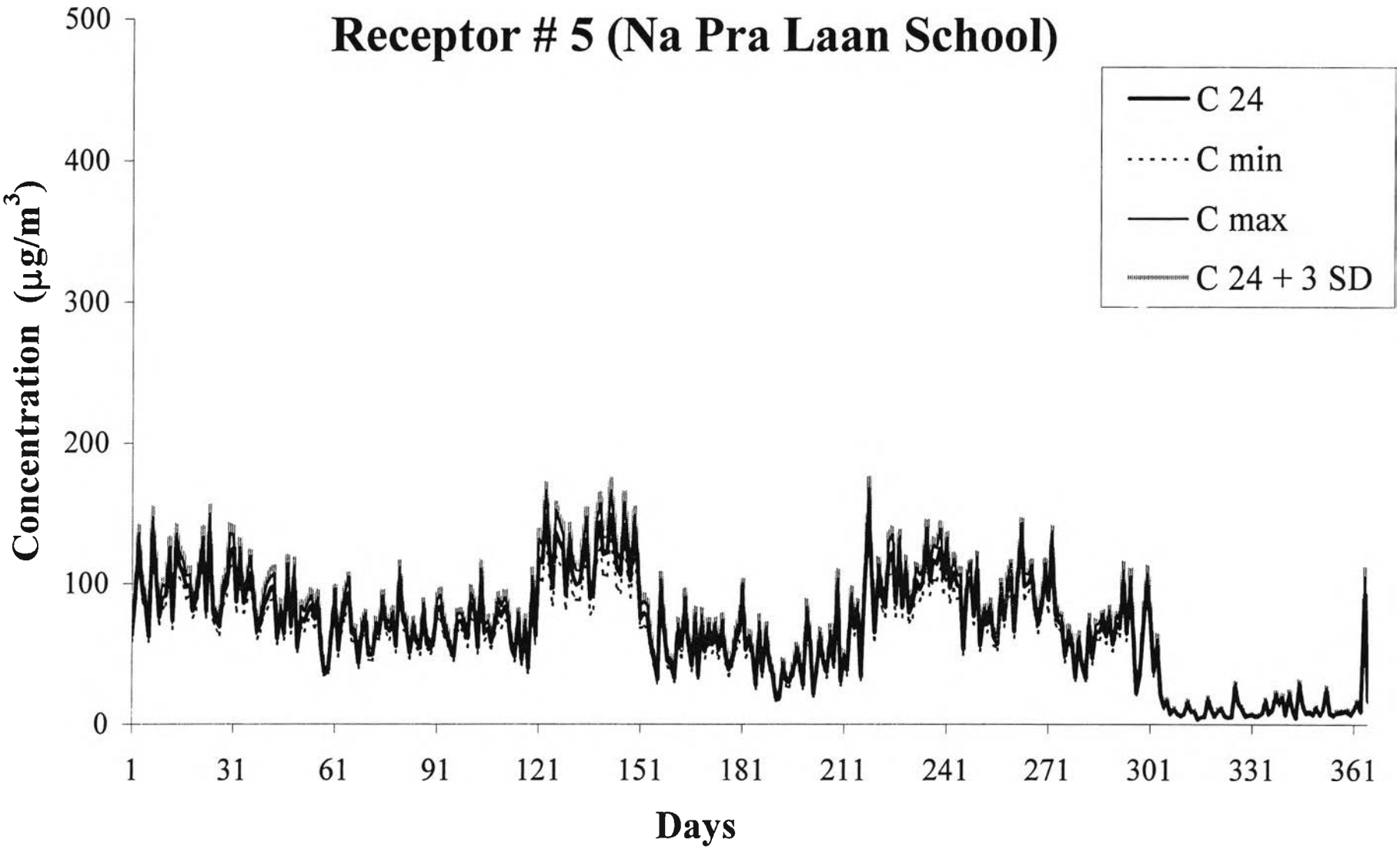

Figure 5.21 Annual trend of the statistical values of 24-hour average concentration of PM_{10} at Na Pra Laan School obtained from modeling with uncertain emission input

5.4 Effect of the Auto-correlation Coefficient (α)

Uncertainty in the meteorological data has been shown to play an important role on the level of uncertainty in the output PM_{10} concentrations. Among the meteorological data, the wind direction and wind speed are known to have a great influence on the atmospheric dispersion of air pollutants. Like most meteorological variables, they are auto-correlated random variables. For example, if the sky is sunny right now, the probability is low that the sky will suddenly become cloudy the next moment or soon. This is referred to as the auto-correlated property of the random variable. The degree of auto correlation is expressed as ($1 - \alpha$) in Equations (4.11) and (4.12), where α is the weighting parameter. The larger the value of α, the lesser the degree of auto-correlation. To test the effect of autocorrelation in the wind direction and the wind speed on the transient behavior of the PM_{10}, the weighting parameter (α) is changed to 0.25 and 0.75, respectively, from the base case value of 0.5. The simulation results are presented and discussed here.

5.4.1 The Case of Wind Speed

Figure 5.22 shows the monthly trend of the predicted 24-hour average values of PM_{10} at Receptor # 1 when the weighting parameter α of the wind direction is varied. The simulation results for the month of January show that the degree of autocorrelation in the wind speed slightly affects the transient behavior of the output PM_{10}. Perhaps, this can be attributed to the calm wind condition of the wind speed input in the study area (wind speed < 2.0 m/s), as shown in Figure 5.10.

5.4.2 The Case of Wind Direction

Figure 5.23 shows the monthly trend of the PM_{10} at Receptor # 1 for the month of January when the weighting parameters of the wind direction is varied. Obviously, the degree of autocorrelation in the wind direction has more effect on the behavior of the PM_{10} concentration than that of the wind speed. Generally speaking, the higher the degree of autocorrelation (small α), the smoother the transient behavior of the output PM_{10}. However, to elucidate the effect of the autocorrelation level on the level of uncertainty in the PM_{10}, it is necessary to carry out Monte-Carlo simulations, which is beyond the scope of the present study.

Generally speaking, the wind speed has a greater effect on the pollutant concentration than the wind direction when a general overview of the pollutant concentration dispersed in a large area is of interest. On the other hand, the wind direction has a greater effect when the pollutant concentration of interest is limited to a specified receptor.

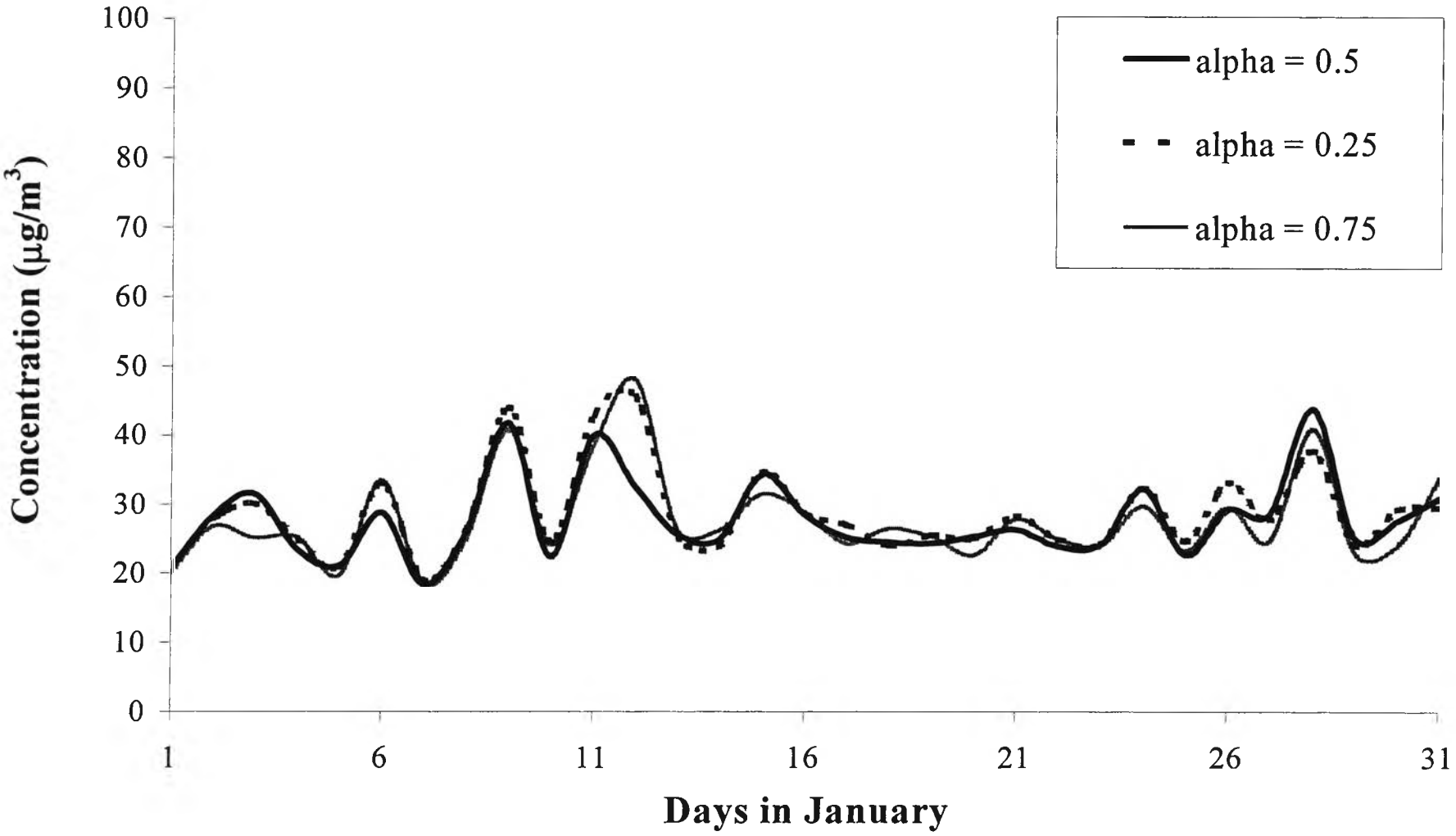

Figure 5.22 Effect of autocorrelation level in the wind speed on the transient behavior of PM_{10} at receptor # 1

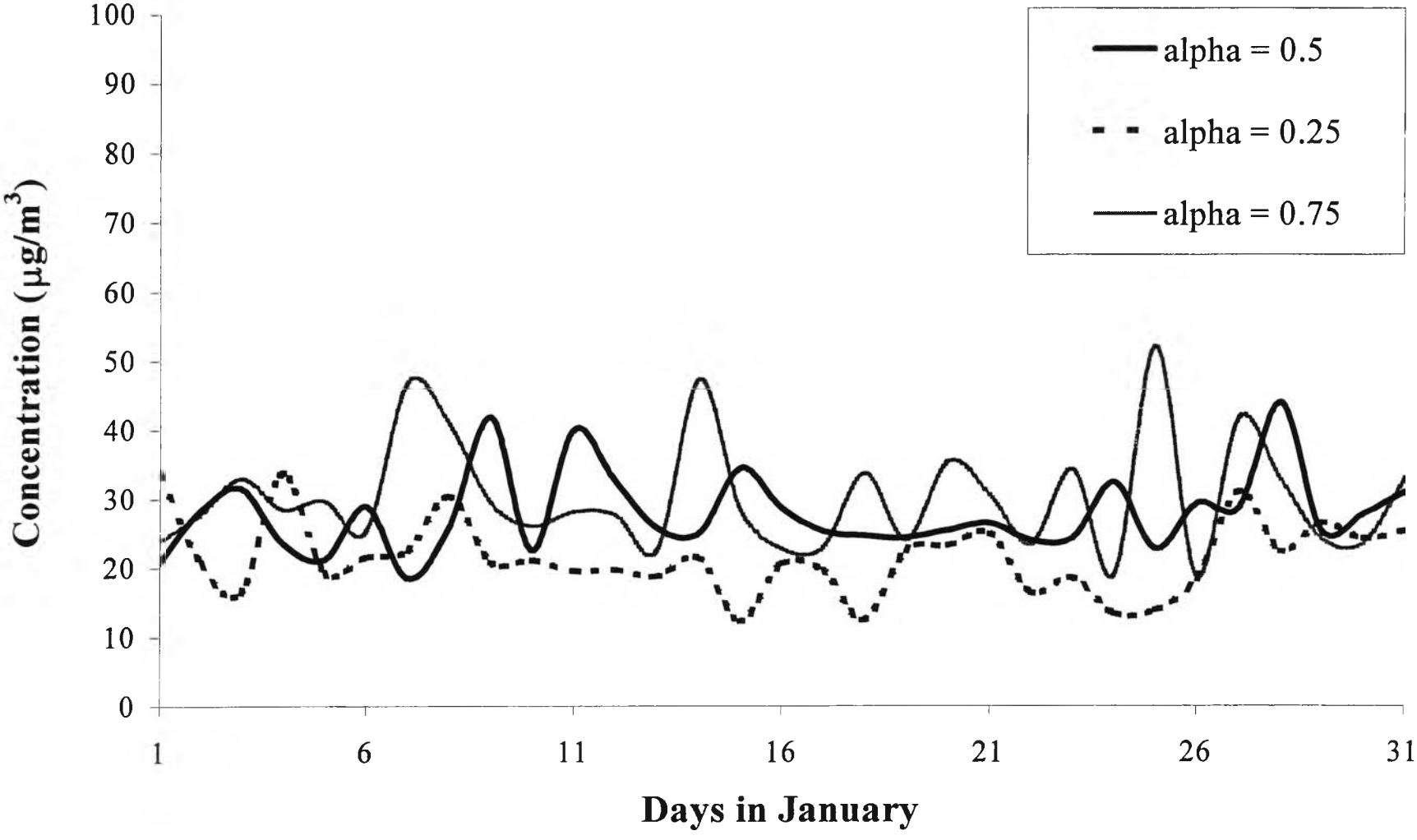

Figure 5.23 Effect of autocorrelation level in the wind direction on the transient behavior of PM_{10} at receptor # 1